edition of the World Health Organization (WHO) guidelines. Five of the 167 patients were not included in this study; three because they received preoperative chemotherapy and two because of the poor quality of the specimens obtained. Thus, 162 patients were ultimately eligible for inclusion in this study, and their median follow-up period was 5.0 years.

Clinical characteristics were retrieved from the clinical records available. The following clinico-pathological factors were assessed retrospectively in relation to immunohistochemical analysis: age (<70 years *vs* ≥70 years), tumor size (≤3 cm *vs* >3 cm), pathological nodal involvement (positive *vs* negative), grade of differentiation (well or moderately differentiated *vs* poorly differentiated), location of the tumor (central *vs* peripheral), vascular invasion (absent *vs* present), lymphatic invasion (absent *vs* present), and pleural invasion (absent *vs* present). Central location of a tumor was defined as a tumor location limited to the trachea, bronchi, or segmental bronchi, and peripheral location as location more peripheral than the subsegmental bronchi. Cumulative smoking was presented by a smoking index, defined as a product of the numbers of cigarette per day and the duration (years).

**Pathological studies and tissue microarray (TMA) construction.** After fixing the specimens with cold methanol and embedding in paraffin, serial 4-μm sections were stained with hematoxylin–eosin (H&E) and by the alcian blue-periodic acid-Schiff method to visualize cytoplasmic mucin and by the Verhoeff-van-Gieson (VvG) method to visualize elastic fibers. Sections stained by the VvG method were examined for the presence of vascular invasion and pleural invasion. The sections were reviewed by two pathologists (Y.S. and G.I.) and the histological diagnoses were based on the revised WHO histological classification.

For microarray construction, the above two pathologists marked morphologically representative tumor areas, avoiding necrotic areas and the area in which cancer cells and stromal cells are intermingled, and definitely containing interfaces between the tumor nests and stroma, on an H&E-stained slide of donor tissue. The TMAs were constructed with a manual tissue-arraying instrument (Azumaya, Tokyo, Japan). The microarray instrument is used to remove a tissue core from the donor block with a thin-walled needle having an inner diameter of approximately 2.0 mm. Core samples were precisely placed in an empty paraffin block (the recipient block) at a specifically assigned location. Two core samples of each tumor were routinely corrected from two different areas. Normal lung tissue from the some patient's specimen was used as a positive control for each staining. Specimens from the 162 cases were punched, and core samples were mounted in the same recipient blocks.

**Immunohistochemical analysis.** TMA recipient blocks were cut into 4-μm sections and mounted on silane-coated slides. After deparaffinizing the sections in xylene and dehydrating them in a graded ethanol series, the slides were washed three times in phosphate-buffered saline (PBS) and immersed in a 0.3% hydrogen peroxide solution in methanol for 15 min. to inhibit endogenous peroxidase activity. The slides were then washed three times in PBS, and nonspecific binding was blocked by preincubation with 2% normal swine serum in PBS (blocking buffer) for 30 min at room temperature. Individual slides were then incubated overnight at 4°C with anti-podoplanin (clone D2-40; Signet, Dedham, MA, USA) at a 1:50 dilution, and anti-CD44 (clone DF1485; Novocastra, Newcastle, UK) at a 1:40 dilution, and anti-p63 (clone 4A4; Dako Cytomation, Carpinteria, CA, USA) at a 1:200 dilution. Finally, the slides were washed three times with PBS and incubated with the EnVision+ System HRP (Dako, Glostrup, Denmark), and the reaction products were stained with diaminobenzidine and counterstained with hematoxylin.

When more than 10% of the tumor cells showed an unequivocally strong reaction with an antibody, the tumor was classified as positive. Cytoplasm and/or membrane immunoreactivity was considered to indicate podoplanin and CD44 expression. p63 expression was considered positive if distinct nuclear staining was present. Moreover, we discriminated between ''peripheral expression pattern'' and ''diffuse expression pattern'' in positive immunoreactivity by the tumor nests with these antibodies. Peripheral expression pattern was defined as cells showing strong expression localized to the periphery of the tumor nests with no or weak expression in the central area. Diffuse expression pattern was defined as a less clear staining intensity between the peripheral and central areas of the tumor nests.

**Statistical analysis.** The associations between immunohistochemical expression status and clinico-pathological parameters were analyzed by using the $\chi^2$-test or Fisher's exact test. Overall survival was measured from the date of surgery to the date of death from any cause or the date on which the patient was last known to be alive. Survival curves were plotted according to the Kaplan–Meier method and compared using the log-rank test. All tests were two-sided, and $P$-values <0.05 were considered statistically significant. The Stat-view 5.0 software package was used to perform the statistical analysis (SAS Institute, Cary, NC, USA).

## Results

**Characteristics of the patients.** The clinico-pathological characteristics of the 162 patients are summarized in Table 1. Male predominance and a high smoking index were outstanding characteristics, and there were only three never smokers. The

**Table 1. Clinico-pathological features of squamous cell carcinoma cases ($n$ = 162)**

| | |
|---|---|
| Gender | |
| Male | 147 |
| Female | 15 |
| Age | |
| Median (range) | 67 (31–84) |
| Smoking index | |
| Median (range) | 960 (0–2760) |
| Tumor size (cm) | |
| Median (range) | 3.8 (1.0–9.4) |
| N Stage | |
| pN0 | 117 |
| pN1/pN2 | 45 |
| Tumor location | |
| Central | 37 |
| Peripheral | 125 |
| Differentiation | |
| Well/moderate | 3/104 |
| Poor | 55 |
| Vascular invasion | |
| Absent | 113 |
| Present | 49 |
| Lymphatic invasion | |
| Absent | 105 |
| Present | 57 |
| Pleural invasion | |
| Absent | 116 |
| Present | 46 |
| Pathological stage | |
| IA | 50 |
| IB | 62 |
| IIA | 13 |
| IIB | 34 |
| IIIA | 3 |

5-year overall survival rate of the 162 patients as a whole was 67.7%.

**Expression of podoplanin, CD44, and p63 by cancer cells and characteristic immunostaining.** We examined the expression of podoplanin, CD44, and p63 by immunohistochemical staining in a series of 162 specimens of SqCC of the lung. Podoplanin and CD44 were expressed mainly in the cytoplasm and membrane of the tumor cells, and p63 was expressed in the nuclei. The results of the immunohistochemical analysis are shown in Figure 1. In normal lung tissue, podoplanin expression was consistently detected in the endothelium of the lymphatic vessels and basal cells in the bronchial epithelium (Fig. 1a). CD44 expression was observed in the basal layer of the bronchial epithelium and peribronchial mesenchymal cells (Fig. 1c), and p63 was expressed in the nuclei of basal cells in the bronchial epithelium (Fig. 1e). The tumor cells in 107 (66%) of the 162 specimens were positive for podoplanin. The tumor cells in 145 (89.5%) were positive for CD44, and the tumor cells in 151 (93.2%) were positive for p63 (Table 2). As discussed, there were two patterns of expression in the cases that immunohistochemically stained podoplanin positive. A total of 102 (95.3%) of the 107 podoplanin-positive cases showed peripheral expression patterns, (Fig. 1b) whereas only five cases (4.7%) showed diffuse expression patterns in the tumor nests. Figure 1(d,f) shows the results for CD44 and p63 staining of the same specimen as in Figure 1b. The CD44 staining pattern was similar to that of

**Table 2. Expression of podoplanin, CD44, and p63 by cancer cells**

| Molecular marker | Negative (%) | Positive (%) |
|---|---|---|
| Podplanin | 55 (34.0) | 107 (66.0) |
| CD44 | 17 (10.5) | 145 (89.5) |
| p63 | 11 (6.8) | 151 (93.2) |

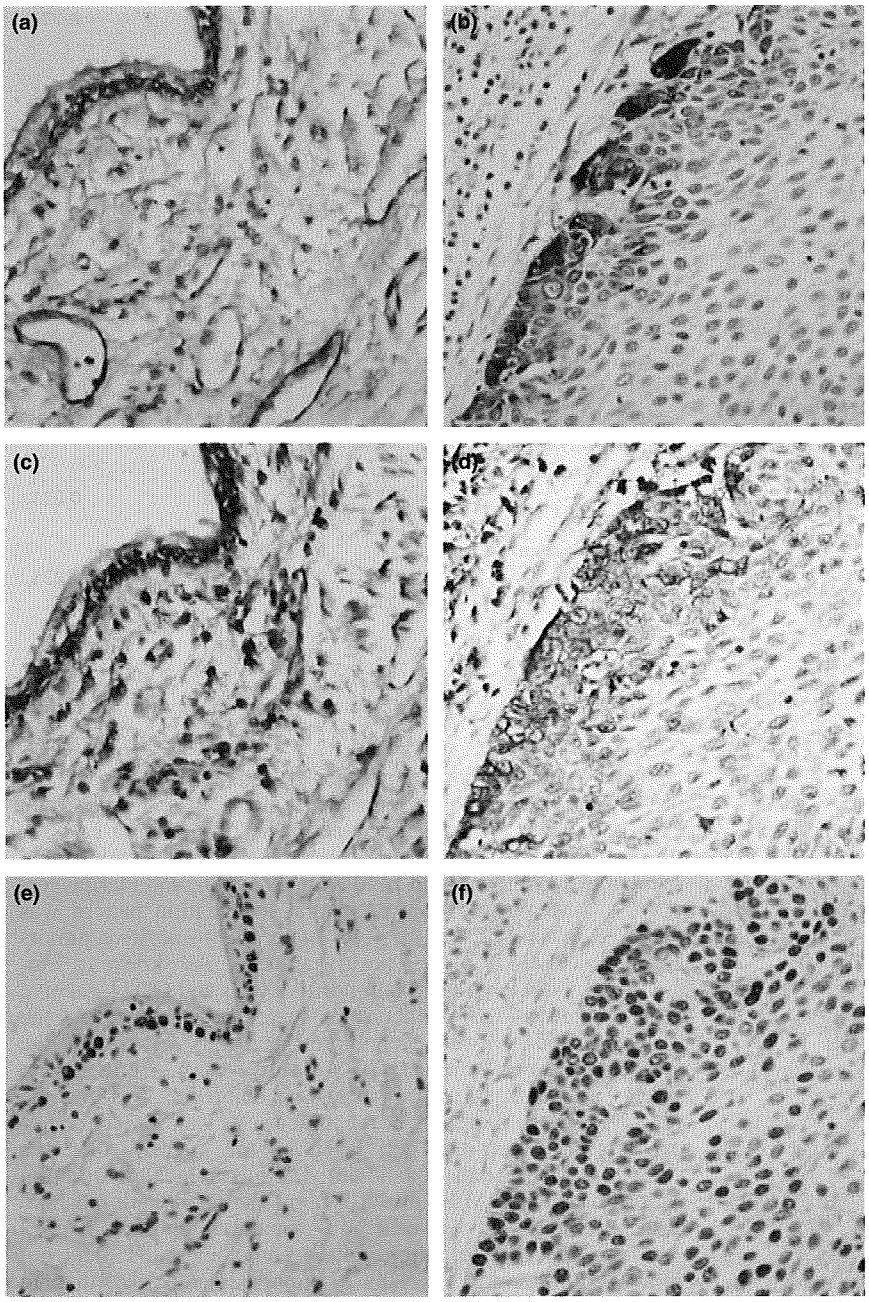


**Fig. 1.** Immunohistochemical analysis of podoplanin, CD44, and p63 expression in squamous cell carcinomas of the lung and a normal part of the specimen from one patient. (a) Podoplanin expression was detected in the endothelium of lymphatic vessels and in bronchial basal cells. (b) Podoplanin expression is mainly localized at the periphery of invading tumor nests. (c) CD44 expression was expressed in the bronchial basal cells. (d) CD44 expression was predominantly found in the peripheral areas of the tumor nests, but its distribution was broader than that of podoplanin. (e) p63 expression was observed in the nuclei of the bronchial basal cells. (f) Difference in p63 expression between the peripheral area and central area was less clear.



doi: 10.1111/j.1349-7006.2009.01295.x

podoplanin, but the area of intense CD44 staining was broader than that of podoplanin. Eighty-one (55.9%) of the CD44-positive cases showed peripheral expression patterns (Fig. 1d), whereas 64 cases (44.1%) showed diffuse expression patterns. In 65 (43%) of the p63-positive cases there were peripheral expression patterns, but the difference in the staining intensity of p63 between the peripheral and central areas was less clear compared with podoplanin and CD44 staining (Fig. 1f).

As shown in Figure 1(b,d,f), the distribution of podoplanin-positive cells appeared to be localized more peripherally within the tumor nests than the distribution of CD44- and p63-positive cells. When CD44 and p63 expressions were compared, p63-positive cell layers were broader compared to CD44-positive cell layers in the tumor nest periphery. We named this expression the "hierarchical distribution pattern" (Fig. 2).

The hierarchical distribution pattern was observed in 95 (88.8%) of the 107 podoplanin-positive cases (Table 3). Of the 12 remaining cases, there were diffuse extensive expression cases of all three markers in five. Further, there were CD44-negative/p63 peripheral staining patterns in two, negative staining cases for both CD44 and p63 in two, negative staining for CD44/diffuse staining pattern for p63 in one, p63-positive cells more restricted to the periphery of the tumor nests than in the CD44-positive cases in one, and CD44-positive cells expressed in only the central area in one.

**Correlation between clinico-pathological features and the hierarchical distribution-positive cases.** Correlations between the hierarchical distribution-positive cases and the clinico-pathological features of the patients are shown in Table 4. The hierarchical distribution-positive cases was significantly associated with the absence of lymphatic invasion ($P = 0.035$). No other clinico-pathological factors were correlated with them.

**The hierarchical distribution cases showed better overall survival.** The 5-year overall survival rate of patients with the podoplanin-positive cases and the podoplanin-negative cases was 74.4% and 54.8%, respectively. Patients with the podoplanin-positive cases had a longer overall survival time than those with the podoplanin-negative cases ($P = 0.018$; Fig. 3a), whereas staining with CD44 and p63 had no prognostic significance ($P = 0.941$ and 0.640, respectively; data not shown). Moreover, we examined the prognostic value of the hierarchical distribution–positive cases and podoplanin-negative cases. The 5-year overall survival rate of the hierarchical distribution–positive cases was 71.7% and the hierarchical distribution-positive cases had a more favorable outcome than podoplanin-negative cases ($P = 0.043$; Fig. 3b).

**Table 3. Characteristic distribution of podoplanin-, CD44-, and p63-positive cells in podoplanin-positive squamous cell carcinoma**

| Podoplanin positive cases ($n$ = 107) | | |
|---|---|---|
| Hierarchical distribution pattern | Diffuse expression pattern | Others |
| 95 (88.8%) | 5 (4.7%) | 7 (6.5%) |

**Table 4. Correlation between clinico-pathological features and the hierarchical distribution–positive cases**

| Variables | Hierarchical distribution cases ($n$ = 95) | Podoplanin-negative cases ($n$ = 55) | $P$-values |
|---|---|---|---|
| Gender | | | |
| Male | 85 | 50 | 0.778 |
| Female | 10 | 5 | |
| Age | | | |
| <70 | 48 | 33 | 0.262 |
| ≧70 | 47 | 22 | |
| Tumor size | | | |
| ≧3cm | 42 | 21 | 0.471 |
| >3 cm | 53 | 34 | |
| N Stage | | | |
| pN0 | 74 | 36 | 0.097 |
| pN1 or pN2 | 21 | 19 | |
| Differentiation | | | |
| Well or moderate | 64 | 34 | 0.491 |
| Poor | 31 | 21 | |
| Location | | | |
| Central | 16 | 15 | 0.128 |
| Peripheral | 79 | 40 | |
| Vascular invasion | | | |
| Absent | 67 | 38 | 0.853 |
| Present | 28 | 17 | |
| Lymphatic invasion | | | |
| Absent | 68 | 30 | 0.035 |
| Present | 27 | 25 | |
| Pleural invasion | | | |
| Absent | 69 | 38 | 0.644 |
| Present | 26 | 17 | |

## Discussion

In this study, we analyzed immunohistochemically the expression of podoplanin, CD44, and p63 in 162 pulmonary SqCCs.

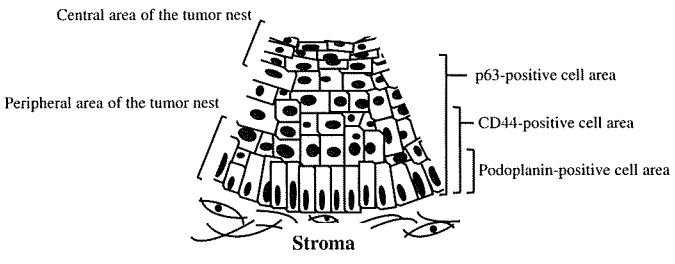


**Fig. 2.** Schema of the hierarchical distribution pattern of podoplanin, CD44, and p63 within tumor nests. The distribution of podoplanin-positive cells appeared to be more localized to the peripheral area of the tumor nests than the distribution of CD44- and p63-positive cells. The distribution of p63-positive cells was broader than that of the CD44-positive cells.

Focusing on the positive expression patterns, in 102 (95.3%) of the 107 podoplanin-positive tumors, tumor cells showing strong expression were localized in the periphery of the tumor nests. A similar pattern of podoplanin expression has been demonstrated immunohistochemically in head and neck, skin, and uterine cervix.[20–23] Meanwhile, this peripheral localization pattern was observed in only 55.9% (81/145) of the CD44-positive tumors and 43% (65/151) of p63-positive tumors. As shown in Figure 1(b,d), both the podoplanin-positive cells and CD44-positive cells resided at the periphery of tumor nests; however, the podoplanin-positive cells were more specifically restricted to the peripheral layers than the CD44-positive cells. Furthermore, when CD44 and p63 expressions were compared, p63-positive cell layers in the periphery of the tumor nests were broader compared to CD44-positive cell layers in the majority of cases (141/145; 97.2%; data not shown). The hierarchical distribution pattern was observed in almost 90% of the podoplanin-positive cases (Table 3). In non-cancerous squamous epithelium also, this hierarchical distribution pattern could be found (data not shown). Furthermore, we have previously reported that in human squamous SqCC cell line A431, almost all cultured

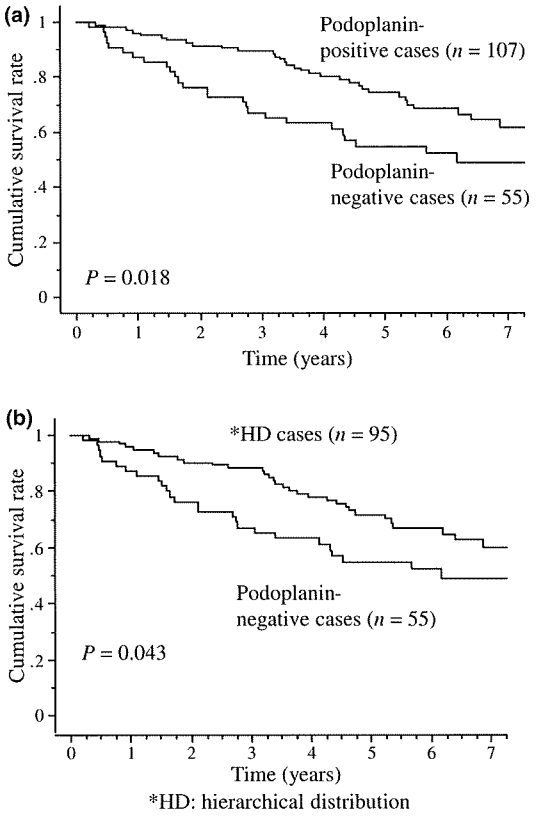


**Fig. 3.** Kaplan–Meier curves for overall survival. Overall survival curves of patients according to whether their tumor was podoplanin-positive or podoplanin-negative. The 5-year overall survival rates of the former and the latter were 74.4% and 54.8%, respectively. Overall survival curves of patients stratified according to whether their tumor was podoplanin-positive with the hierarchical distribution pattern or podoplanin-negative. The 5-year overall survival rates of the former and the latter were 71.7% and 54.8%, respectively.

A431 cells were positive for CD44 whereas the frequency of podoplanin-positive cells was approximately 35% in flow cytometric analysis.[6] This finding implies that podoplanin-positive A431 cells are a limited subpopulation of CD44-positive cells under *in vitro* condition, and is compatible with our immunohistochemical results. Considering a morphological representative for the developmental hierarchy based on the CSC hypothesis, podoplanin expression would reflect the most immature CSC status in its differentiation process, and podoplanin may be a marker of cells with a capacity for further maturation of SqCC. On the other hand, CD44 expression reflects even more differentiated cells of SqCC, and p63 expression may broadly reflect the CSC differentiation process ranging from immature CSC status to mature cells.

In the current study, podoplanin immunoreactivity had a prognostic significance, and this result is compatible with our previous study limited to pathological stage IB SqCC.[20] Furthermore it is notable that patients who had podoplanin-positive tumors with the hierarchical distribution pattern had significantly better overall survival than those who had podoplanin-negative tumors. Additionally these tumors showed a significant correlation of the absence of lymphatic invasion and had a certain tendency to no lymph node metastasis. These results suggest that SqCC with the hierarchical distribution pattern may indicate lower biological aggressiveness. It seems possible that SqCC showing the hierarchical distribution pattern is a well-organized tumor group based on the CSC concept, whereas SqCC with an unclear hierarchy is a disordered tumor group in terms of the developmental hierarchy.

In this study, 55 cases (34%) of SqCC were podoplanin-negative. This type of SqCC may fall into the following categories. First, CSCs of podoplanin-negative SqCC are enriched in the subpopulation expressing molecular markers other than podoplanin. Second, such cases may be a kind of tumor with no hierarchical structure based on the CSC concept. Some cancers contain small subpopulations of cancer-initiating cells, whereas others contain common tumorigenic cells with little evidence of hierarchical organization.[24] Podoplanin-negative SqCC might be the latter type of carcinoma. It will be important to analyze the biological features of podoplanin-negative pulmonary SqCCs in order to understand SqCC biology.

We examined the human SqCC cell lines, TE3, TE4, and TE10 other than A431, and the frequency of podoplanin expressing cells was 100%, 100%, and 0.5%, respectively (Atsumi *et al*, unpublished data). Given the expression frequencies in these SqCC cell lines, whether the podoplanin-positive cells can always represent a CSC subpopulation in a variety of SqCCs will remain a matter of debate.

CD44 is transmembrane hyaluronan receptor, and its cytoplasmic region, comprising 72 amino acid residues, has been shown to associate with actin filaments in various cells, a process mediated by ERM (ezrin/radixin/moesin) proteins.[25] Villar *et al.* demonstrated that the cytoplasmic domain of podoplanin also binds ERM proteins to promote epithelial–mesenchymal transition.[25] Considering the similar localization of podoplanin- and CD44-positive cells within the tumor nests and their common signaling via ERM proteins, it might be possible to think that signaling via Podoplanin and CD44 collectively mediate to express the biological properties of CSC .

Targeting CSCs has been proposed as an effective approach to cancer treatment, because CSCs are thought to be insensitive to conventional treatments and to be responsible for relapses. From this standpoint, the realization of CSCs due to a specific molecular marker, podoplanin, may lead to a new treatment strategy for SqCC.

## Acknowledgments

The technical support of Hiroko Hashimoto, Manabu Yamazaki, and Shinya Yanagi is gratefully acknowledged. This study was supported in part by a Grant-in-Aid for Cancer Research (19-10) from the Ministry of Health, Labour, and Welfare of Japan, and a Grant-in-Aid for the Third Term Comprehensive 10-year Strategy for Cancer Control from the Ministry of Health, Labour, and Welfare of Japan.

## Disclosure Statement

No potential conflicts of interest are disclosed.

## References

1 Fukuoka M, Yano S, Giaccone G *et al.* Multi-institutional randomized phase II trial of gefitinib for previously treated patients with advanced non-small-cell lung cancer (The IDEAL 1 Trial) [corrected]. *J Clin Oncol* 2003; **21**: 2237–46.

2 Chang A, Parikh P, Thongprasert S *et al.* Gefitinib (IRESSA) in patients of Asian origin with refractory advanced non-small cell lung cancer: subset analysis from the ISEL study. *J Thorac Oncol* 2006; **1**: 847–55.

3 Shepherd FA, Rodrigues Pereira J, Ciuleanu T *et al.* Erlotinib in previously treated non-small-cell lung cancer. *N Engl J Med* 2005; **353**: 123–32.



doi: 10.1111/j.1349-7006.2009.01295.x

4 Peacock CD, Watkins DN. Cancer stem cells and the ontogeny of lung cancer. *J Clin Oncol* 2008; **26**: 2883–9.
5 Weissman IL, Anderson DJ, Gage F. Stem and progenitor cells: origins, phenotypes, lineage commitments, and transdifferentiations. *Ann Rev Cell Dev Biol* 2001; **17**: 387–403.
6 Atsumi N, Ishii G, Kojima M, Sanada M, Fujii S, Ochiai A. Podoplanin, a novel marker of tumor-initiating cells in human squamous cell carcinoma A431. *Biochem Biophys Res Commun* 2008; **373**: 36–41.
7 Pellegrini G, Dellambra E, Golisano O *et al.* p63 identifies keratinocyte stem cells. *Proc Natl Acad Sci USA* 2001; **98**: 3156–61.
8 Prince ME, Sivanandan R, Kaczorowski A *et al.* Identification of a subpopulation of cells with cancer stem cell properties in head and neck squamous cell carcinoma. *Proc Natl Acad Sci USA* 2007; **104**: 973–8.
9 Kahn HJ, Marks A. A new monoclonal antibody, D2-40, for detection of lymphatic invasion in primary tumors. *Lab Invest* 2002; **82**: 1255–7.
10 Kaneko MK, Kato Y, Kitano T, Osawa M. Conservation of a platelet activating domain of Aggrus/podoplanin as a platelet aggregation-inducing factor. *Gene* 2006; **378**: 52–7.
11 Martin-Villar E, Scholl FG, Gamallo C *et al.* Characterization of human PA2.26 antigen (T1alpha-2, podoplanin), a small membrane mucin induced in oral squamous cell carcinomas. *Int J Cancer* 2005; **113**: 899–910.
12 Weber GF, Bronson RT, Ilagan J, Cantor H, Schmits R, Mak TW. Absence of the CD44 gene prevents sarcoma metastasis. *Cancer Res* 2002; **62**: 2281–6.
13 Fasano M, Sabatini MT, Wieczorek R, Sidhu G, Goswami S, Jagirdar J. CD44 and its v6 spliced variant in lung tumors: a role in histogenesis? *Cancer* 1997; **80**: 34–41.
14 Mylona E, Giannopoulou I, Fasomytakis E *et al.* The clinicopathologic and prognostic significance of CD44+/CD24(-/low) and CD44-/CD24+ tumor cells in invasive breast carcinomas. *Hum Pathol* 2008; **39**: 1096–102.
15 Boldrup L, Coates PJ, Gu X, Nylander K. DeltaNp63 isoforms regulate CD44 and keratins 4, 6, 14 and 19 in squamous cell carcinoma of head and neck. *J Pathol* 2007; **213**: 384–91.
16 Irwin MS, Kaelin WG. p53 family update: p73 and p63 develop their own identities. *Cell Growth Differ* 2001; **12**: 337–49.
17 Wang BY, Gil J, Kaufman D, Gan L, Kohtz DS, Burstein DE. P63 in pulmonary epithelium, pulmonary squamous neoplasms, and other pulmonary tumors. *Hum Pathol* 2002; **33**: 921–6.
18 Yang A, McKeon F. P63 and P73: P53 mimics, menaces and more. *Nat Rev* 2000; **1**: 199–207.
19 Hibi K, Trink B, Patturajan M *et al.* AIS is an oncogene amplified in squamous cell carcinoma. *Proc Natl Acad Sci USA* 2000; **97**: 5462–7.
20 Ito T, Ishii G, Nagai K *et al.* Low podoplanin expression of tumor cells predicts poor prognosis in pathological stage IB squamous cell carcinoma of the lung, tissue microarray analysis of 136 patients using 24 antibodies. *Lung Cancer.* 2008; **3**: 418–24.
21 Yuan P, Temam S, El-Naggar A *et al.* Overexpression of podoplanin in oral cancer and its association with poor clinical outcome. *Cancer* 2006; **107**: 563–9.
22 Durchdewald M, Guinea-Viniegra J, Haag D *et al.* Podoplanin is a novel fos target gene in skin carcinogenesis. *Cancer Res* 2008; **68**: 6877–83.
23 Dumoff KL, Chu CS, Harris EE *et al.* Low podoplanin expression in pretreatment biopsy material predicts poor prognosis in advanced-stage squamous cell carcinoma of the uterine cervix treated by primary radiation. *Mod Pathol* 2006; **19**: 708–16.
24 Quintana E, Shackleton M, Sabel MS, Fullen DR, Johnson TM, Morrison SJ. Efficient tumour formation by single human melanoma cells. *Nature* 2008; **456**: 593–8.
25 Martin-Villar E, Megias D, Castel S, Yurrita MM, Vilaro S, Quintanilla M. Podoplanin binds ERM proteins to activate RhoA and promote epithelial-mesenchymal transition. *J Cell Sci* 2006; **119**: 4541–53.

Lung Cancer 63 (2009) 418–424

Contents lists available at ScienceDirect

Lung Cancer

journal homepage: www.elsevier.com/locate/lungcan

# Low podoplanin expression of tumor cells predicts poor prognosis in pathological stage IB squamous cell carcinoma of the lung, tissue microarray analysis of 136 patients using 24 antibodies

Takeo Ito[a,b,c], Genichiro Ishii[a], Kanji Nagai[b], Tatsuya Nagano[a,b], Masakazu Kojika[a,b], Yukinori Murata[a], Naho Atsumi[a], Yutaka Nishiwaki[b], Eishi Miyazaki[c], Toshihide Kumamoto[d], Atsushi Ochiai[a,*]

[a] Pathology Division, Research Center for Innovative Oncology, National Cancer Center Hospital East, 6-5-1, Kashiwanoha, Kashiwa, Chiba, Japan
[b] Thoracic Oncology Division, National Cancer Center Hospital East, Kashiwa, Chiba, Japan
[c] Division of Pulmonary Disease, Department of Brain and Nerve Science, Oita University Faculty of Medicine, Oita, Japan
[d] Division of Neurology and Neuromuscular Disorders, Department of Brain and Nerve Science, Oita University Faculty of Medicine, Oita, Japan

ARTICLE INFO

*Article history:*
Received 15 January 2008
Received in revised form 20 April 2008
Accepted 10 June 2008

*Keywords:*
Stage IB
Squamous cell carcinoma
Lung cancer
Prognosis
Podoplanin
D2-40
Tissue microarray
Immunohistochemistry

ABSTRACT

The aim of this study was to identify clinicopathological and biological prognostic markers for patients who had undergone complete resection of pathological stage IB squamous cell carcinoma (SqCC) of the lung. A total of 136 consecutive stage IB SqCC patients fulfilled eligibility criteria, and their clinicopathological factors were evaluated. Tissue microarrays were also constracted, and immunohistochemical staining with 24 antibodies was performed. Correlations between clinicopathological factors, antibody immunohistochemical reactions, the patients' overall survival (OS) and relapse-free survival (RFS) were evaluated. The univariate analysis showed that 70-year-old and over elderly group had a shorter OS time and RFS time than the younger group ($p = 0.0086$ and $p = 0.0091$, respectively). The univariate analysis for immunohistochemical staining showed that the podoplanin-negative group had a shorter OS time and RFS time than the podoplanin-positive group ($p = 0.0106$ and $p = 0.0308$, respectively). Multivariate analysis revealed a significant correlation between both the 70-year-old and over elderly group and the podoplanin-negative group and poor outcome (OS, $p = 0.007$ and $p = 0.008$, respectively; RFS, $p = 0.008$ and $p = 0.024$, respectively). The results showed that patient age and a novel biological prognostic marker, podoplanin, are useful for predicting a poor outcome of patients after complete resection of stage IB SqCC of the lung.


## 1. Introduction

Non-small-cell lung cancer (NSCLC) is the leading cause of cancer deaths all over the world, and complete surgical resection is generally recognized as the most effective local treatment for early stage NSCLC. Approximately one third of NSCLC patients undergo surgical resection with curative intent, however, despite surgical resection approximately 20% of pathological (p-) stage IA, 40% of p-stage IB NSCLC patients die within 5 years [1].

Adenocarcinoma and squamous cell carcinoma (SqCC) are the two major histopathological subtypes of NSCLC, and they have different pathogenetic pathways and distinct biological characteristics. Although many reports have described prognostic markers for NSCLC or adenocarcinoma, there have been few reports in regard to SqCC [2–5]. Also, there are a considerable number of new treatment options for adenocarcinoma, including gefitinib, erlotinib, and bevacizumab, but the efficacy of gefitinib and erlotinib against SqCC is inadequate, and SqCC subtype is considered a contraindication for use of bevacizumab because of the high incidence of bleeding events [6–10]. Therefore, the development of effective treatment for SqCC is an urgent task for pulmonary oncologists.

Some large-scale clinical trials of adjuvant chemotherapy demonstrated that adjuvant platinum-based chemotherapy improves the 5-year survival rate of patients after complete resection of NSCLC [11–13]. However, none of these trials demonstrated a significant survival benefit in stage IB patients. Although tegafur-uracil has been established as an effective oral adjuvant chemotherapeutic drug for stage IB NSCLC, no survival benefit for the SqCC subgroup has been demonstrated [14,15]. In their guideline for adjuvant therapy for NSCLC, the joint expert panel of Cancer Care Ontario Program in Evidence-Based Care and the American Society of Clinical Oncology does not recommend adjuvant cisplatin-based chemotherapy for routine use for patients after complete resection for stage IB NSCLC [16].

* Corresponding author. Tel.: +81 4 7134 6855; fax: +81 4 7134 6865.
*E-mail address:* aochiai@east.ncc.go.jp (A. Ochiai).

0169-5002/$ – see front matter © 2008 Elsevier Ireland Ltd. All rights reserved.
doi:10.1016/j.lungcan.2008.06.008

Identifying the group of stage IB patients with a worse prognosis based on the presence of prognostic markers may make it possible to provide them with the maximum benefit of adjuvant chemotherapy or to identify molecular targets for SqCC. We therefore adopted p-stage IB SqCC patients as our study population in this study and attempted to identify prognostic factors in a series of 136 patients. We then analyzed the prognostic significance of clinicopathological factors and biomarkers in regard to overall and relapse-free survival.

## 2. Materials and methods

### 2.1. Patient selection

During the period between June 1993 and December 2005, a total of 3396 patients underwent surgical resection for primary lung cancer at the National Cancer Center Hospital East, Chiba, Japan, and we reviewed the 146 consecutive p-stage IB SqCC patients. All patients signed the Institutional Review Board-approved informed consent form. The tumors were staged according to the International Union Against Cancer's tumor-node-metastasis (TNM) classification, and histologically subtyped and graded according to the third edition of the World Health Organization (WHO) guidelines. We excluded 10 patients from this study: 5 patients in whom wedge or partial resection was performed because of poor pre-operative pulmonary function, 2 patients who received pre-operative chemotherapy, 2 patients in whom resection was incomplete, and 1 patient who received adjuvant chemotherapy. Ultimately, 136 patients were selected for further study, and their median follow-up time was 1336 days (range, 32–4687) (Table 1).

### 2.2. Pathological studies

The specimens were fixed with 10% formalin or cold methanol and embedded in paraffin. Serial 4 μm sections were stained with Hematoxylin and Eosin (H&E) and by the alcian blue-periodic acid-Schiff method, to detect cytoplasmic mucin production, and by the elastic van Gieson method, for elastic fibers. The sections were reviewed by two pulmonary pathologists (T.I. and G.I.) according to the histological criteria in the WHO classification. If tumor cells were identified in the lumen of a blood vessel or lymphatic vessel, vascular or lymphatic vessel invasion was judged to be positive. Pleural invasion was judged to be positive if tumor cells had invaded the elastic layer of the visceral pleura or beyond. In cases of disagreement they discussed it with multi-headed microscope until an agreement was reached.

**Table 1**
Patient and tumor characteristics ($n = 136$)

| | | |
|---|---|---|
| Gender | Male | 117 |
| | Female | 19 |
| Age | Median (range) | 71 (31–88) |
| Smoking index | Median (range) | 930 (0–2800) |
| Tumor size | Median (range) | 4.5 (1.6–11.9) |
| Tumor side | Right | 84 |
| | Left | 52 |
| Upper lobe located tumor | Yes | 58 |
| | No | 78 |
| Operation | Lobectomy/bilobectomy | 130/4 |
| | Pneumonectomy | 2 |
| Differentiation | Well/moderately | 8/83 |
| | Poorly | 45 |
| Vascular invasion | (−) | 36 |
| | (+) | 100 |
| Lymphatic vessel invasion | (−) | 105 |
| | (+) | 31 |
| Pleural invasion | (−) | 85 |
| | (+) | 51 |

### 2.3. Evaluation of clinicopathologic factors

Clinical characteristics were extracted based on the clinical records available. The following clinicopathologic factors were assessed retrospectively to investigate their impact on survival; gender, age (<70 years vs. ≥70 years), smoking index (<900 vs. ≥900), greatest tumor dimension (<5 cm vs. ≥5 cm), laterality of the tumor (right vs. left), upper lobe location (upper vs. non-upper), grade of differentiation (well or moderately differentiated vs. poorly differentiated), vascular invasion (positive vs. negative), lymphatic vessel invasion (positive vs. negative), pleural invasion (positive vs. negative).

### 2.4. Construction of tumor tissue microarrays (TMA)

The most representative tumor areas, avoiding necrotic areas in order to evaluate as many tumor cells as possible, were carefully selected and marked on the H&E stained slide of donor tissue for construction of microarrays. TMAs were constructed with a manual tissue-arraying instrument (Azumaya, Tokyo, Japan). The microarray system consists of thin-walled stainless-steel needle having an internal diameter of approximately 2 mm and a stylet for transferring and removing the contents of the needle. Core samples were retrieved from donor tissue blocks and precisely arrayed in a new (recipient) paraffin block. Specimens were routinely sampled by taking two core samples of each tumor in different areas. A normal control tissue microarray (fixed with 10% formalin or cold methanol) that includes non-malignant specimens from various organs, including placenta and a malignant melanoma specimen, was used as a positive control for each staining. Specimens from the 136 cases were punched, and core samples were mounted in the same recipient blocks.

### 2.5. Antibodies and immunohistochemical staining

Twenty-four molecular markers were selected for investigation in this study. These included markers for cell cycle-related proteins, growth factors and hormone receptors, cellular adhesion molecules, tumor stem cell markers, hypoxia-induced proteins, oncofetal proteins, mesothelioma-related proteins, and others. The antibodies used for these markers in this study are listed in Table 2. Immunohistochemical staining was performed as follows. TMA recipient blocks were cut into 4 μm sections and mounted on silane-coated slides, with the initial sections H&E stained to verify histology. The sections were deparaffinized in xylene and dehydrated in a graded alcohol series, and endogenous peroxidase was blocked with 3% hydrogen peroxide in absolute methyl alcohol. Heat-induced epitope retrieval was performed for 20 min at 95 °C with a 0.02 mol/L concentration of citrate buffer (pH 6.0). After allowing the slides to cool at room temperature for 60 min, they were rinsed with deionized water and incubated overnight with primary antibodies. The slides were then washed three times with phosphate-buffered saline and incubated with the EnVision + System-HRP (DAKO, Glostrup, Denmark). The reaction products were stained with diaminobenzidine and counterstained with Hematoxylin.

**Table 2**
Antibodies used

| Classification/antibody | Clone | Pretreatment | Dilution | Source |
|---|---|---|---|---|
| Cell cycle-related proteins | | | | |
| Cyclin B1 | 7A9 | Microwave | 1:20 | Novocastra |
| Cyclin D1 | Polyclonal | Microwave | 1:400 | Santa Cruz |
| Growth factors and hormone receptors | | | | |
| EGFR | EGFR. 25 | Microwave | 1:50 | Novocastra |
| IGFR | 24-31 | Microwave | 1:100 | Chemicon International |
| c-erbB2 | CB11 | Microwave | Prediluted | Ventana Medical Systems |
| ER | 6F11 | Microwave | Prediluted | Ventana Medical Systems |
| PgR | 1A6 | Microwave | Prediluted | Ventana Medical Systems |
| Cellular adhesion molecules | | | | |
| Beta-catenin | 14 | Microwave | 1:200 | Becton Dickinson Biosciences |
| E-cadherin | 36 | Microwave | 1:100 | Becton Dickinson Biosciences |
| CD44 | DF1485 | Microwave | 1:40 | Novocastra |
| CD56 | Lu243 | Microwave | Prediluted | Ventana Medical Systems |
| Tumor stem cell markers | | | | |
| CD133 | AC133 | Microwave | 1:200 | Miltenyi Biotec |
| p63 | 4A4 | Microwave | 1:200 | DakoCytomation |
| c-kit | Polyclonal | Microwave | 1:50 | DakoCytomation |
| Hypoxia-induced proteins | | | | |
| CA IX | Polyclonal | Microwave | 1:150 | Santa Cruz |
| GLUT-1 | Polyclonal | Microwave | 1:200 | Thermo Fischer Scientific |
| Oncofetal proteins | | | | |
| AFP | Polyclonal | Microwave | 1:1000 | Dakopatts |
| Beta-hCG | Polyclonal | Microwave | 1:1000 | Dakopatts |
| PLAP | 8A9 | Microwave | 1:50 | DakoCytomation |
| MAGE | 6C1 | Microwave | 1:100 | Santa Cruz |
| Mesothelioma-related markers | | | | |
| Podoplanin | D2-40 | Microwave | 1:50 | Covance |
| Calretinin | Polyclonal | Microwave | 1:50 | Zymed Laboratories |
| Others | | | | |
| BCRP | BXP-21 | Microwave | 1:20 | Chemicon International |
| p53 | DO-7 | Microwave | 1:50 | DakoCytomation |

EGFR: epidermal growth factor receptor; IGFR: insulin-like growth factor-1 receptor; ER: estrogen receptor; PgR: progesterone receptor; CA IX: carbonic anhydrase IX; GLUT-1: glucose transporter-1; AFP: alpha fetoprotein; beta-hCG: beta-chain of human chorionic gonadotropin; PLAP: placental alkaline phosphatase; MAGE: melanoma associated antigen; BCRP: breast cancer resistance protein.

### 2.6. Identification of positive cases

The cases were evaluated in random order with no knowledge of the patient's history. When more than 10% of the cancer cells reacted positively with an antibody, they were recorded as positive, except for beta-catenin and E-cadherin. Beta-catenin staining of the cytoplasm and cytoplasmic membrane and/or nucleus was assessed independently. E-cadherin staining of the cytoplasm and cytoplasmic membrane was assessed. When more than 80% of the cancer cells reacted positively with beta-catenin and E-cadherin, they were recorded as positive.

### 2.7. Statistical analysis

Calculations were performed with SPSS II software (SPSS, Chicago, IL, USA). Correlations between clinicopathologic factors and immunohistochemical reactions were evaluated by Pearson's Chi-square test. We defined overall survival (OS) time as the period from the day of tumor resection to the day of the patient's death, and relapse-free survival (RFS) time as the period from the day of tumor resection to the day tumor relapse was confirmed (based on symptoms and physical examination or based on clinical imaging), or to the day of the patient's death. Survival curves were plotted according to the Kaplan–Meier method, and differences between the curves were analyzed by the log-rank test. The Cox proportional hazard regression model was used to perform the multivariate analysis. Statistical differences were considered significant if the $p$-value was less than 0.05.

## 3. Results

### 3.1. Clinicopathological factors

The 3-year OS rate and RFS rate of the 136 patients as a whole was 82.4 and 73.5%, respectively. The profiles of the patients in regard to gender, age, smoking index, tumor size, tumor site, operation procedure, histological differentiation category, vascular invasion, lymphatic vessel invasion, and pleural invasion status are summarized in Table 1. Male predominance and high smoking status were outstanding characteristics. There were only 4 never smokers in this population. The univariate analysis showed that the 70-year-old and over elderly patient group had a shorter OS time and RFS time than the younger group ($p = 0.0086$, 0.0091, respectively; Table 3 and Fig. 2A and B). No other clinicopathological factors have prognostic significance.

### 3.2. Biological markers

Since no clinicopathologic factors except age were significant, we attempted to identify biological markers that would be of prognostic value in IB SqCC. EGFR, IGFR, beta-catenin (cytoplasm and cytoplasmic membrane expression), E-cadherin, CD44, and p63

were positive in over 90% of the patients, and c-erb B2/HER2, ER, PgR, beta-catenin (nuclear expression), CD56, AC133, AFP, beta-hCG, and PLAP were negative in over 95% of the patients.

Podoplanin staining was interpreted as positive in 69 of the 136 (51%) tumors. Podoplanin-positive cells were predominantly found in the peripheral layers of tumor nests, but weak or not at all in keratinized layers. The stromal lymphatic vessels of podoplanin-negative patients were stained positive as an internal positive control (Fig. 1A and B). In contrast, carbonic anhydrase IX (CA IX) expression was predominantly found around areas of necrosis and in a layer 1–6 cells in thickness away from necrosis, whereas more distant cellular layers did not express CA IX (Fig. 1C and D). Evaluation of the relation between podoplanin staining status and clinicopathological factors revealed significantly more cases of poorly differentiated SqCC in the podoplanin-negative group ($p = 0.045$; Table 4). According to the univariate analysis, the podoplanin-negative group had a shorter OS time and RFS time than the podoplanin-positive group ($p = 0.0106$ and $p = 0.0308$, respectively; Table 3 and Fig. 2C and D). Staining with the CA IX and other antibodies used in this study had no prognostic significance. We evaluated patients age and podoplanin status versus patients' OS and RFS by multivariate analysis, and the results showed significant correlations between both the 70-year-old and over elderly group and podoplanin-negative group and outcome (OS, $p = 0.007$ and $p = 0.008$, respectively; RFS, $p = 0.008$ and $p = 0.024$, respectively; Table 5).

**Table 3**
Univariate analyses of clinicopathological factors and biological markers

| Variables | Number of patients | % | os, *p*-value | RFS, *p*-value |
|---|---|---|---|---|
| Clinicopathological factors | | | | |
| Male gender | 117 | 86 | N.S. | N.S. |
| Age ≥ 70 years | 74 | 54 | 0.0086 | 0.0091 |
| Smoking index > 900 | 72 | 53 | N.S. | N.S. |
| Tumor size > 5 cm | 43 | 32 | N.S. | N.S. |
| Tumor site = right | 84 | 62 | N.S. | N.S. |
| Non-upper lobe located tumor | 78 | 57 | 0.1326 | 0.1731 |
| Differentiation = poorly | 45 | 33 | N.S. | N.S. |
| v (+) | 100 | 74 | N.S. | N.S. |
| ly (+) | 31 | 23 | N.S. | N.S. |
| p (+) | 51 | 38 | 0.0943 | 0.0533 |
| Biological markers | | | | |
| Cyclin B1 (+) | 91 | 67 | N.S. | N.S. |
| Cyclin D1 (+) | 85 | 63 | N.S. | N.S. |
| EGFR (+) | 136 | 100 | N.S. | N.S. |
| IGFR (+) | 123 | 90 | N.S. | N.S. |
| c-erbB2 (+) | 2 | 1 | N.S. | N.S. |
| ER (+) | 0 | 0 | N.S. | N.S. |
| PgR (+) | 0 | 0 | N.S. | N.S. |
| Beta-catenin | | | | |
| Cytoplasmic membrane (+) | 134 | 99 | N.S. | N.S. |
| Nucleus (+) | 2 | 1 | N.S. | N.S. |
| E-cadherin (+) | 131 | 96 | N.S. | N.S. |
| CD44 (+) | 130 | 96 | N.S. | N.S. |
| CD56 (+) | 5 | 4 | N.S. | N.S. |
| CD133 (+) | 0 | 0 | N.S. | N.S. |
| p63 (+) | 127 | 93 | N.S. | N.S. |
| c-kit (+) | 20 | 15 | N.S. | N.S. |
| CA IX (+) | 70 | 51 | N.S. | N.S. |
| GLUT-1 (+) | 79 | 58 | N.S. | N.S. |
| AFP (+) | 1 | 1 | N.S. | N.S. |
| Beta-hCG (+) | 2 | 2 | N.S. | N.S. |
| PLAP (+) | 2 | 2 | N.S. | N.S. |
| MAGE (+) | 57 | 42 | N.S. | N.S. |
| Podoplanin (−) | 67 | 49 | 0.0106 | 0.0308 |
| Calretinin (+) | 53 | 39 | N.S. | N.S. |
| BCRP (+) | 67 | 49 | N.S. | N.S. |
| p53 (+) | 49 | 36 | N.S. | N.S. |

OS: overall survival; RFS: relapse-free survival; N.S.: not significant; v: vascular invasion; ly: lymphatic vessel invasion; p: pleural invasion; EGFR: epidermal growth factor receptor; IGFR: insulin-like growth factor-1 receptor; ER: estrogen receptor; PgR: progesterone receptor; CA IX: carbonic anhydrase IX; GLUT-1: glucose transporter-1; AFP: alpha fetoprotein; beta-hCG: beta-chain of human chorionic gonadotropin; PLAP: placental alkaline phosphatase; MAGE: melanoma associated antigen; BCRP: breast cancer resistance protein.

**Table 4**
Correlation between clinicopathological factors and podoplanin immunoreactivity

| Variables | Podoplanin immunoreactivity | | *p*-Value |
|---|---|---|---|
| | (+) | (−) | |
| Gender | | | 0.808 |
| Male | 60 | 57 | |
| Female | 9 | 10 | |
| Age (years) | | | 1.000 |
| <70 | 31 | 31 | |
| ≥70 | 38 | 36 | |
| Smoking index | | | 0.865 |
| <900 | 33 | 31 | |
| ≥900 | 36 | 36 | |
| Tumor size (cm) | | | 0.581 |
| <5 | 34 | 27 | |
| ≥5 | 35 | 40 | |
| Tumor site | | | 1.000 |
| Right | 43 | 41 | |
| Left | 26 | 26 | |
| Upper lobe located tumor | | | 0.864 |
| Yes | 28 | 30 | |
| No | 39 | 39 | |
| Differentiation | | | 0.045 |
| Well-moderately | 52 | 39 | |
| Poorly | 17 | 28 | |
| Vascular invasion | | | 0.439 |
| (−) | 16 | 20 | |
| (+) | 53 | 47 | |
| Lymphatic vessel invasion | | | 0.416 |
| (−) | 51 | 54 | |
| (+) | 18 | 13 | |
| Pleural invasion | | | 0.292 |
| (−) | 40 | 45 | |
| (+) | 29 | 22 | |

N.S.: Not significant.

## 4. Discussion

We adopted p-stage IB pulmonary SqCC patients as the subject of this study in order to exclude very early stage patients and lymph node metastasis-positive patients. The results did not reveal any useful clinicopathological prognostic factors for p-stage IB pulmonary SqCC in this series except patient age. However, podoplanin, which is a mesothelioma-related marker, was identified as a significant prognostic biological marker for p-stage IB pulmonary SqCC.

Vascular or pleural invasion is generally considered an indicator of a poor prognosis in surgically resected NSCLC patients [17,18]. Funai et al. [5], on the other hand, reported age and *N* classification as independent prognostic factors for peripheral-type pulmonary SqCC and that vascular invasion and pleural invasion are not. Although vascular invasion was frequently observed (74%) in the present study, no significant prognostic value was demonstrated. These findings are consistent with those reported by Funai, and suggest that no clinicopathologic factors predict the outcome after surgical resection for p-stage IB pulmonary SqCC.

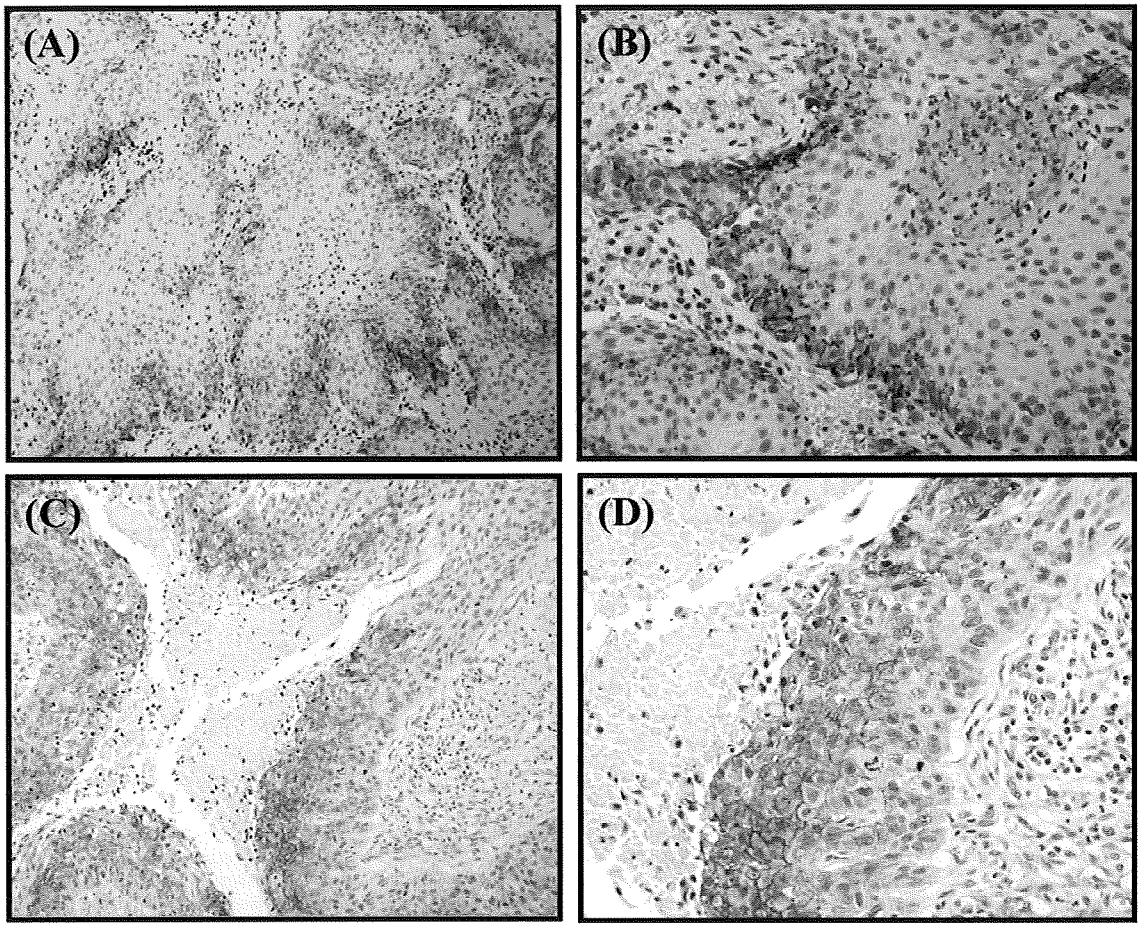


**Fig. 1.** Immunohistochemical staining pattern of podoplanin and carbonic anhydrase IX (CA IX) in a positive case. (A) Podoplanin-positive cells were predominantly found in the peripheral areas of tumor nests. (B) High power view of subpart (A). (C) CAIX expression was predominantly found around areas of necrosis and in a layer 1–6 cells in thickness away from necrosis. (D) High power view of subpart (C).

CAIX has been reported to be a prognostic marker for resected pulmonary SqCC. Giatromanolaki et al. [19] noted that CAIX expression by surgically resected pulmonary SqCC correlated with a poor outcome. By contrast, our results showed that CAIX expression was not related to a poor outcome in p-stage IB pulmonary SqCC patients, but the expression characteristics were similar to those reported by Giatromanolaki. The subjects of his study were p-stage T1-2, N0-1 patient, and the difference in stages may have been responsible for the inconsistency with our results.

Human podoplanin (T1alpha-2, aggrus and gp36) is a type-1 transmembrane sialomucin-like glycoprotein [20]. Because podoplanin is expressed on the lymphatic vessel endothelium and not on blood vessel endothelium, it is widely used in histopathology as a specific marker for lymphatic endothelium. On the other hand, enhanced podoplanin expression has been shown in SqCC itself, including in the lung [21], head and neck [22], and uterine cervix [23]. The cells that were positive for podoplanin in the present study were predominantly found in peripheral layers of tumor nests, but weak or not at all in keratinized layers. A similar pattern of expression has been reported in SqCC of the uterine cervix and of the head and neck [22,23]. In well differentiated squamous cell carcinoma, we can observe various differentiated cells from basal layer "immature" cells to keratinized "terminally differentiated" cells, imitating normal squamous epithelium. Since podoplanin-positive cells were observed in the peripheral layers of tumor nests but weak in keratinized layers, podoplanin-positive squamous cell carcinoma may reserve developmental hierarchy. On the other hand, in poorly differentiated squamous cell carcinoma, tumor cells are generally homogenous and the developmental hierarchy is unclear. Based on these concepts, podoplanin may be a marker of cells with capacity of further maturation of squamous cell carcinoma.

Kunita et al. [24] recently reported that podoplanin contributed to the establishment of pulmonary metastasis by Chinese hamster ovary cells by promoting platelet aggregation. This finding suggests that podoplanin-expressing tumors have more malignant characteristics, which is consistent with the evidence of correla-

**Table 5**
Multivariate analysis of the clinicopathological and biological markers

| Variable | Overall survival | | Relapse-free survival | |
|---|---|---|---|---|
| | HR (95% CI) | *p*-Value | HR (95% CI) | *p*-Value |
| Age ≥ 70 years | 2.328 (1.263–4.289) | 0.007 | 2.182 (1.228–3.875) | 0.008 |
| Podoplanin | 2.288 (1.240–4.223) | 0.008 | 1.917 (1.091–3.369) | 0.024 |

HR: Hazard ratio; CI: confidence interval.

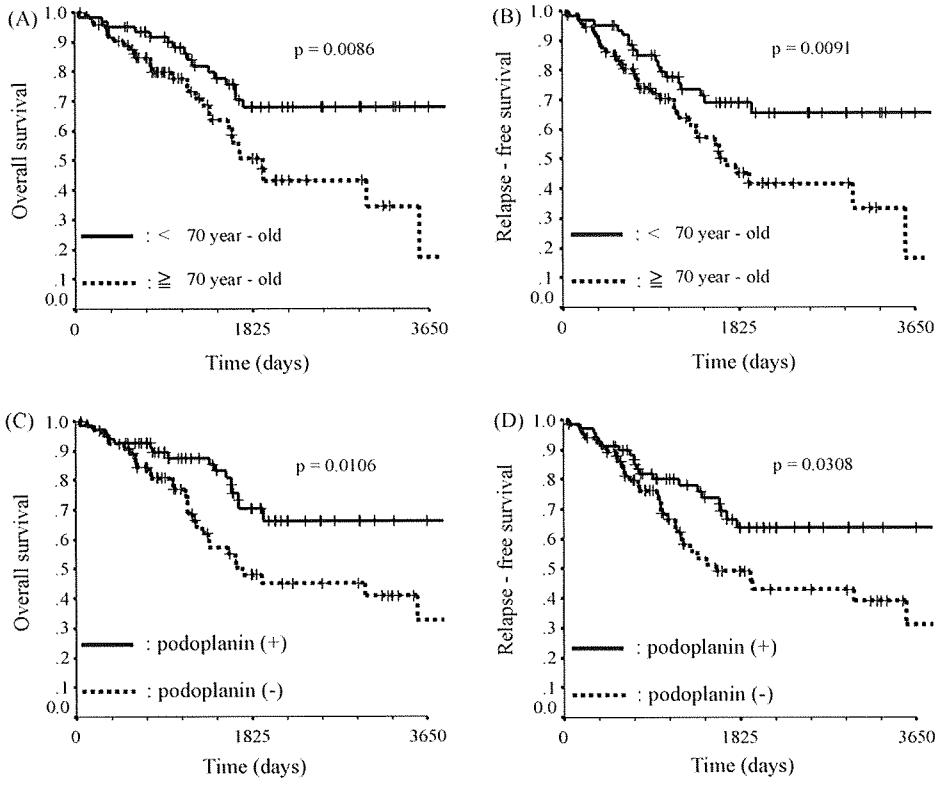


**Fig. 2.** Kaplan–Meier curves for overall survival and relapse-free survival. (A) Overall and (B) relapse-free survival curve stratified for <70-year-old and ≥70-year-old patients. The 3-year overall survival rate of the <70-year-old group and ≥70-year-old group was 88.0 and 77.7%, respectively. The 3-year relapse-free survival rate of the <70-year-old group and ≥70-year-old group was 77.6 and 70.3%, respectively. (C) Overall and (D) relapse-free survival curve stratified for podoplanin-positive vs. negative patients. The 3-year overall survival rate of the podoplanin-positive group and-negative group was 87.6 and 77.0%, respectively. The 3-year relapse-free survival rate of the podoplanin-positive group and-negative group was 80.2 and 66.5%, respectively.

tion between high podoplanin immunoreactivity in SqCC of the head and neck and both lymph node metastasis and a shorter disease-specific survival [22]. By contrast, Dumoff et al. [23] showed correlations between low podoplanin immunoreactivity in SqCC of the uterine cervix correlated and lymphatic invasion, lymph node metastasis, and a shorter recurrence-free survival. Our results show correlations between low podoplanin immunoreactivity in p-stage IB pulmonary SqCC and poor differentiation, shorter OS time and RFS time, similar to the findings in SqCC of the uterine cervix [23]. There were several possible reasons for this contradiction. The epithelial counterpart of SqCC has generally been considered to be different in the head and neck, uterine cervix, and lung. The source of head and neck SqCC is squamous epithelium or dysplastic squamous epithelium and podoplanin expression is observed in basal cell layer of normal squamous epithelium of head and neck. So podoplanin expression of squamous cell carcinoma of head and neck may reflect its biological characteristics of basal cell. On the other hand, SqCC of the uterine cervix is thought to arise by squamous metaplasia of endocervial mucinous epithelium, which is not originally squamous epithelium. Normally, there is no squamous epithelium in the lower respiratory tract or lung, and the exact source of pulmonary SqCC is still unknown. Then the role of podoplanin for squamous cell carcinoma at these sites may be different from head and neck, and influences clinical outcome inversely. Alternatively, platelet aggregation promoting metastases may not be a main way of establishing pulmonary SqCC metastases. Although we could not evaluate association between podoplanin expression and lymph node metastases for an association because of patient selection, podoplanin expression was not correlated with lymphatic vessel invasion or vascular invasion in our study. Also, we investigated the number of lymphatic vessels in the tumor core samples, however, no significant correlation was observed between the number of lymphatic vessels and podoplanin expression (data not shown). Moreover, we investigated the difference of clinical characteristics of relapse between podoplanin-negative and positive groups. However, there was no significant difference between the type (site) of relapse and podoplanin expression (data not shown). Further investigations of podoplanin function in pulmonary SqCC are anticipated.

In conclusion, the only conventional clinicopathological marker that was useful for predicting poor outcome of p-stage IB pulmonary SqCC patients after complete resection was patient age, however, a novel biological prognostic marker, podoplanin, was identified. Patients after complete resection of pathological stage IB squamous cell carcinoma of the lung with low podoplanin expression status are expected poor outcome. Prospective study with a larger number of patients is warranted to confirm the benefit of adjuvant chemotherapy for these patients.

## Conflict of interest

None declared.

## Acknowledgements

The technical support of Mai Okumoto, Kimihiko Kawamura and Manabu Yamazaki and clinical advice of Akikazu Kawase, Syuji Ohta, Kenji Takahashi and Jun-ichi Nitadori are gratefully acknowledged.

*Grant support*: This study was supported in part by a Grant-in-Aid for Cancer Research (19-10) from the Ministry of Health, Labour, and Welfare of Japan and a Grant-in-Aid for the Third Term Comprehensive 10-year Strategy for Cancer Control from the Ministry of Health, Labour, and Welfare of Japan.

## References

[1] Goya T, Asamura H, Yoshimura H, Kato H, Shimokata K, Tsuchiya R, et al. Prognosis of 6644 resected non-small cell lung cancers in Japan: a Japanese lung cancer registry study. Lung Cancer 2005;50:227–34.
[2] Wu S, Sato M, Endo C, Sakurada A, Dong B, Aikawa H, et al. hnRNP B1 protein may be a possible prognostic factor in squamous cell carcinoma of the lung. Lung Cancer 2003;41:179–86.
[3] Werle B, Lotterle H, Schanzenbacher U, Lah TT, Kalman E, Kayser K, et al. Immunochemical analysis of cathepsin B in lung tumours: an independent prognostic factor for squamous cell carcinoma patients. Br J Cancer 1999;81:510–9.
[4] Villegas FR, Coca S, Villarrubia VG, Jimenez R, Chillon MJ, Jareno J, et al. Prognostic significance of tumor infiltrating natural killer cells subset CD57 in patients with squamous cell lung cancer. Lung Cancer 2002;35:23–8.
[5] Funai K, Yokose T, Ishii G, Araki K, Yoshida J, Nishimura M, et al. Clinicopathologic characteristics of peripheral squamous cell carcinoma of the lung. Am J Surg Pathol 2003;27:978–84.
[6] Fukuoka M, Yano S, Giaccone G, Tamura T, Nakagawa K, Douillard JY, et al. Multi-institutional randomized phase II trial of gefitinib for previously treated patients with advanced non-small-cell lung cancer (The IDEAL 1 Trial) [corrected]. J Clin Oncol 2003;21:2237–46.
[7] Nishiwaki Y, Yano S, Tamura T, Nakagawa K, Kudoh S, Horai T, et al. Subset analysis of data in the Japanese patients with NSCLC from IDEAL 1 study on gefitinib. Gan To Kagaku Ryoho 2004;31:567–73.
[8] Chang A, Parikh P, Thongprasert S, Tan EH, Perng RP, Ganzon D, et al. Gefitinib (IRESSA) in patients of Asian origin with refractory advanced non-small cell lung cancer: subset analysis from the ISEL study. J Thorac Oncol 2006;1:847–55.
[9] Shepherd FA, Rodrigues Pereira J, Ciuleanu T, Tan EH, Hirsh V, Thongprasert S, et al. Erlotinib in previously treated non-small-cell lung cancer. N Engl J Med 2005;353:123–32.
[10] Johnson DH, Fehrenbacher L, Novotny WF, Herbst RS, Nemunaitis JJ, Jablons DM, et al. Randomized phase II trial comparing bevacizumab plus carboplatin and paclitaxel with carboplatin and paclitaxel alone in previously untreated locally advanced or metastatic non-small-cell lung cancer. J Clin Oncol 2004;22:2184–91.
[11] Arriagada R, Bergman B, Dunant A, Le Chevalier T, Pignon JP, Vansteenkiste J. Cisplatin-based adjuvant chemotherapy in patients with completely resected non-small-cell lung cancer. N Engl J Med 2004;350:351–60.
[12] Winton T, Livingston R, Johnson D, Rigas J, Johnston M, Butts C, et al. Vinorelbine plus cisplatin versus observation in resected non-small-cell lung cancer. N Engl J Med 2005;352:2589–97.
[13] Douillard JY, Rosell R, De Lena M, Carpagnano F, Ramlau R, Gonzales-Larriba JL, et al. Adjuvant vinorelbine plus cisplatin versus observation in patients with completely resected stage IB-IIIA non-small-cell lung cancer (Adjuvant Navelbine International Trialist Association [ANITA]): a randomised controlled trial. Lancet Oncol 2006;7:719–27.
[14] Kato H, Ichinose Y, Ohta M, Hata E, Tsubota N, Tada H, et al. A randomized trial of adjuvant chemotherapy with uracil-tegafur for adenocarcinoma of the lung. N Engl J Med 2004;350:1713–21.
[15] Hamada C, Tanaka F, Ohta M, Fujimura S, Kodama K, Imaizumi M, et al. Meta-analysis of postoperative adjuvant chemotherapy with tegafur-uracil in non-small-cell lung cancer. J Clin Oncol 2005;23:4999–5006.
[16] Pisters KM, Evans WK, Azzoli CG, Kris MG, Smith CA, Desch CE, et al. Cancer Care Ontario and American Society of clinical oncology adjuvant chemotherapy and adjuvant radiation therapy for stages I–IIIA resectable non-small-cell lung cancer guideline. J Clin Oncol 2007.
[17] Suzuki K, Nagai K, Yoshida J, Nishimura M, Takahashi K, Yokose T, et al. Conventional clinicopathologic prognostic factors in surgically resected non-small cell lung carcinoma. A comparison of prognostic factors for each pathologic TNM stage based on multivariate analyses. Cancer 1999;86:1976–84.
[18] Shimizu K, Yoshida J, Nagai K, Nishimura M, Ishii G, Morishita Y, et al. Visceral pleural invasion is an invasive and aggressive indicator of non-small cell lung cancer. J Thorac Cardiovasc Surg 2005;130:160–5.
[19] Giatromanolaki A, Koukourakis MI, Sivridis E, Pastorek J, Wykoff CC, Gatter KC, et al. Expression of hypoxia-inducible carbonic anhydrase-9 relates to angiogenic pathways and independently to poor outcome in non-small cell lung cancer. Cancer Res 2001;61:7992–8.
[20] Martin-Villar E, Scholl FG, Gamallo C, Yurrita MM, Munoz-Guerra M, Cruces J, et al. Characterization of human PA2.26 antigen (T1alpha-2, podoplanin), a small membrane mucin induced in oral squamous cell carcinomas. Int J Cancer 2005;113:899–910.
[21] Kato Y, Kaneko M, Sata M, Fujita N, Tsuruo T, Osawa M. Enhanced expression of Aggrus (T1alpha/podoplanin), a platelet-aggregation-inducing factor in lung squamous cell carcinoma. Tumour Biol 2005;26:195–200.
[22] Yuan P, Temam S, El-Naggar A, Zhou X, Liu DD, Lee JJ, et al. Overexpression of podoplanin in oral cancer and its association with poor clinical outcome. Cancer 2006;107:563–9.
[23] Dumoff KL, Chu C, Xu X, Pasha T, Zhang PJ, Acs G. Low D2-40 immunoreactivity correlates with lymphatic invasion and nodal metastasis in early-stage squamous cell carcinoma of the uterine cervix. Mod Pathol 2005;18:97–104.
[24] Kunita A, Kashima TG, Morishita Y, Fukayama M, Kato Y, Tsuruo T, et al. The platelet aggregation-inducing factor aggrus/podoplanin promotes pulmonary metastasis. Am J Pathol 2007;170:1337–47.

# Novel spliced form of a lens protein as a novel lung cancer antigen, Lengsin splicing variant 4

Munehide Nakatsugawa,[1,2] Yoshihiko Hirohashi,[1,9] Toshihiko Torigoe,[1,9] Hiroko Asanuma,[1,3] Akari Takahashi,[4] Satoko Inoda,[1] Kenji Kiriyama,[1] Emiri Nakazawa,[4] Kenji Harada,[5] Hideo Takasu,[5] Yasuaki Tamura,[1] Kenjiro Kamiguchi,[1] Noriharu Shijubo,[1,6] Ryoichi Honda,[7] Naohiro Nomura,[8] Tadashi Hasegawa,[3] Hiroki Takahashi[2] and Noriyuki Sato[1]

[1]Department of Pathology, [2]The Third Department of Internal Medicine, [3]Division of Clinical Pathology, Sapporo Medical University School of Medicine, South-1, West-17, Chuo-ku Sapporo 060-8556, [4]Japan Science and Technology Agency, Innovation Plaza Hokkaido, North-19, West-11, Kita-ku, Sapporo, 060-0819, [5]Dainippon Sumitomo Pharma Co., Ltd, Osaka 541-0045, [6]Sapporo Railway Hospital, North-3, East-1, Chuo-ku, Sapporo 060-0033, [7]Sapporo Tokushukai Hospital, Sakaedori 18-chome, Shiroishi-ku, Sapporo 003-0021, [8]Kitahiroshima Hospital, Sakaemachi 1-chome, Kitahiroshima 061-1133, Japan

(Received March 2, 2009/Revised April 8, 2009/Accepted April 8, 2009/Online publication May 19, 2009)

**A glutamine synthetase I family protein, Lengsin, was previously identified as a novel lens-specific transcript in the vertebrate eye. In this report, we show for the first time that Lengsin is a novel tumor-associated antigen expressed ectopically in lung cancer. Interestingly, a novel spliced form of human Lengsin termed 'splicing variant 4', gaining exon 3 that codes extra 63 amino acids, is the dominant transcript form in lung cancer cells. Lengsin mRNA could be detected in 7 of 12 (58%) lung cancer cell lines and 7 of 7 (100%) surgically resected lung cancer tissues. On the other hand, Lengsin transcripts could not be detected in normal major tissues or in other cancer cell lines, including melanoma, colorectal carcinoma, breast carcinoma and hepatocellular carcinoma. In addition, knockdown of Lengsin mRNA with RNAi caused cell death and a decrease of cell viability, suggesting that Lengsin has some essential role in cell survival. Since the lens is an immune-privileged site, we regard Lengsin as a highly immunogenic cancer antigen. Anti-Lengsin autoantibodies were detectable in sera of lung cancer patients, although these patients did not show any lens-related disturbances. Hence, Lengsin splicing variant 4 might be an immunogenic lung cancer-specific antigen that is suitable as a diagnostic marker and for molecular targeting therapy, including immunotherapy. (*Cancer Sci* 2009; 100: 1485–1493)**

Lung cancer is one of the most common malignancies and has high mortality rates in industrial countries.[1] Despite recent progress in chemotherapeutic, radiotherapeutic and surgical treatments, the five-year survival rate of lung cancer patients still remains low, especially in advanced cases. Recently, it was reported that antigen-specific cancer immunotherapy had a partial antitumor effect against lung cancer, and that antigen-specific cancer immunotherapy might be a possible novel treatment for the disease.[2,3] However, candidates for potent immunogenic lung cancer antigens are few at present, and exploitation of such immunogenic lung cancer antigens is highly needed.

Several methods to identify tumor-associated antigens (TAAs) have been reported; among them, microarray screening is a powerful tool to screen tumor-specific genes.[4] We identified several genes expressed preferentially in cancer tissues, but not in normal tissues, with gene chip microarray screening using the GeneChip Human Genome U133 Array Set (Affymetrix, Inc., Santa Clara, CA), which contains approximately 39 000 genes. With this screening, we isolated several genes, including Lengsin, that were overexpressed ectopically and specifically in lung cancers. Lengsin, in the glutamine synthetase I (GSI) superfamily, was previously reported to be a constitutive lens-specific protein with unknown function, although some studies suggested it might have chaperone-like activity.[5–7]

In this study, to evaluate the potency of Lengsin as a molecular target for immunotherapy of lung cancer, we examined expression profiles of Lengsin in lung cancers and normal tissues. We also analyzed cell viability in Lengsin knockdown cells and anti-Lengsin autoantibodies in sera from lung cancer patients. Taken together, our present data suggest that Lengsin may act as a novel immunogenic tumor antigen in lung cancer. We will discuss the immunobiological significance of the lens-related antigen in ocular disease and cancer immunotherapy.

## Materials and Methods

**Human cell lines and culture media.** Lung adenocarcinoma cell lines LHK2 and LNY1 and breast carcinoma cell line HMC2 were established in our laboratory. Lung squamous cell carcinoma cell lines Sq-1 and Sq-19, lung adenocarcinoma cell lines 1-87 and 11-18, lung large cell carcinoma cell line 86-2 and lung small cell carcinoma cell lines Lu65, S2 and LK79, were obtained from the Cell Resource Center for Biomedical Research, Tohoku University (Sendai, Japan). Colon carcinoma cell line HCT15, pancreatic carcinoma cell lines PK8, PK45, CFPAC and Panc-1 were kind gifts from Dr K Imai (Sapporo, Japan). Lung small cell carcinoma cell line Lc817 and hepatocellular carcinoma line CHC32 were purchased from the Japanese Cancer Research Resources Bank (Osaka, Japan). Colon carcinoma cell line KM12LM was a kind gift from Dr K Itoh (Kurume, Japan). Colon carcinoma cell lines Colo205 and WiDr, lung adenocarcinoma cell line A549, breast carcinoma cell line MCF7 and embryonic kidney cell line HEK293T were purchased from American Type Culture Collection (Manassas, VA). Melanoma cell lines 888mel and 1102mel were kind gifts from Dr FM Marincola (National Cancer Institute, Bethesda, MD). All of these cells were cultured in 90% DMEM (Sigma-Aldrich, St. Louis, MO) with 10% heat-inactivated fetal bovine serum (Filtron, Brooklyn, NSW, Australia) at 37°C in a humidified 5% $CO_2$ atmosphere.

**Tissue and serum samples.** Seven pairs of lung cancers and the corresponding non-neoplastic lung tissues were obtained from surgically resected tissues removed at Kushiro City General Hospital. The histological types of the seven cancer tissues were: squamous cell carcinoma, cases #1, #4, #7; adenocarcinoma, cases #2, #5, #6; and large cell carcinoma, case #3. Thirty-four formalin-fixed, paraffin-embedded lung adenocarcinoma tissues for immunohistochemical staining were obtained from surgically resected specimens at Sapporo Medical University Hospital. Forty-two serum samples for enzyme-linked immunosorbent assay (ELISA) were collected from 23 lung cancer patients and 19 healthy donors at Sapporo Medical University Hospital,

[9]To whom correspondence should be addressed. E-mail: hirohash@sapmed.ac.jp or torigoe@sapmed.ac.jp

doi: 10.1111/j.1349-7006.2009.01187.x

Sapporo Railway Hospital, Sapporo Tokushukai Hospital and Kitahiroshima Hospital. Tumor staging was determined according to the UICC classification.[8] We obtained informed consent from all patients and healthy donors according to the guidelines of the Declaration of Helsinki.

**RT-PCR analysis.** Human Multiple Tissue cDNA Panels I and II, and the Human Fetal Multiple Tissue cDNA Panel (Clontech, Mountain View, CA, USA) were used as templates of normal tissue cDNA and normal fetal tissue cDNA. Total RNA was isolated from cultured cells and tumor tissues using the RNeasy Mini Kit (Qiagen, Hilden, Germany). cDNAs were synthesized as described previously.[9] PCR amplification was done in 20 μL of PCR mixture containing 0.25 μL of the cDNA mixture, 0.1 μL of Taq DNA polymerase (Qiagen), and 12 pmol of primers. The PCR mixture was initially incubated at 94°C for 2 min, followed by 35 cycles of denaturation at 94°C for 15 s, annealing at 60°C for 30 s and extension at 72°C for 30 s. We designed two primer pairs for specific detection of Lengsin. The sequences of primer pair I were 5′-CCCTGCTTTCTGCTTTCATC-3′ as a sense primer and 5′-AATAACGCTTTCGGCAGCTA-3′ as an antisense primer. The expected size of the PCR product with primer pair I was 507 bp. The sequences of primer pair II were 5′-GGGAGAAA CGGATATGTCCA-3′ as the sense primer and 5′-CAGTCAC AGTGAAGGTATCA-3′ as the antisense primer. The expected size of the PCR product with primer pair II for Lengsin_wild type (Lengsin_wt) was 395 bp and that for Lengsin splicing variant 4 (Lengsin_vt4) was 584 bp. As an internal control, G3PDH expression was detected using sense primer 5′-ACCACAGTCCATGCCATCAC-3′ and antisense primer 5′-TCCACCACCCTGTTGCTGTA-3′ with an expected PCR product of 452 bp.

**Western blot analysis and immunohistochemical staining.** Western blot analysis using mouse antihuman Lengsin mAb clone #517 (established in our laboratory) was performed as described previously.[10]

Immunohistochemical staining was done on formalin-fixed, paraffin-embedded sections as described previously.[11]

**Small interfering RNA transfection.** Lengsin small interfering RNA (siRNA) duplexes were designed and synthesized using the BLOCK-it RNAi designer system (Invitrogen, Palo alto, CA, USA). The oligonucleotide encoding Lengsin siRNA was 5′-CCTAATGCCAGAGTTATCAACCTTT-3′. It targeted a common sequence between Lengsin_wt and Lengsin_vt4 transcripts. Cells were seeded at 50% confluence, and transfections were carried out using Lipofectamine 2000 (Invitrogen) in Opti-MEM according to the manufacturer's instructions.

**WST-1 assay.** WST-1 assay (Wako Chemicals, Osaka, Japan) was performed according to manufacturer's instructions. Forty-eight hours after post transfection of Lengsin siRNA, the cells were seeded in 96-well flat-bottomed plates ($1 \times 10^4$ in 100 μL of culture medium per well) followed by an additional 72-h incubation. Then, 10 μL of WST-1 solution was added into each wells, and the plates were incubated at 37°C for another 2 h. Absorbance was measured by a microplate reader at a wavelength of 450 nm with a reference wavelength of 655 nm. Each experiment was done independently in triplicate.

**Flow cytometry.** Five days after siRNA transfection, the cells were harvested and washed with PBS, followed by fixation with 70% ethanol overnight at –20°C. After washing with PBS, the cells were re-suspended in PBS containing 250 μg/mL RNase A (Sigma-Aldrich) for 30 min at 37°C and stained with 50 μg/mL propidium iodide (PI) (Invitrogen) for 10 min at 4°C in the dark. To calculate the percentage of cells in the sub-G1 phase, the results were analyzed by flow cytometry (FACS Calibur, Becton-Dickinson, Franklin Lakes, NJ) with CellQuest software analysis. The apoptotic cell rate was determined as the percentage of cells in the sub-G1 phase.

**ELISA.** Preparation of purified recombinant Lengsin was performed according to the method described previously.[12] To coat a 96-well plate with capture protein, purified recombinant Lengsin was diluted in 50 mM bicarbonate buffer (pH 9.5) to a final protein concentration of 5 μg/mL and placed in each well of the 96-well plates (Corning, NY) and incubated overnight at 4°C. After removing antigen solutions and three washes with PBS including 0.05% Tween 20 (PBS–T), plates were blocked with 1% BSA in PBS for 2 h at room temperature (RT). After emptying the wells and three washes with PBS–T, 100 μL of serum sample diluted (1:100) in PBS–T including 0.5% of BSA was added to each well and incubated for 1 h at RT. Then, samples were removed and the wells were washed three times with PBS–T, followed by incubation for 30 min with two thousand dilution of rabbit antihuman IgG conjugated with horseradish peroxidase (Dako, Carpinteria, CA). After removing the antibody solution, the wells were washed three times with PBS–T, then each well was developed with ABTS peroxidase substrate (KPL, Gaithersburg, MD). After incubation for 15 min, absorbance was measured at a wavelength of 405 nm.

**Statistical analysis.** A Student's *t*-test was used to compare two groups. $P < 0.05$ was considered significant.

## Results

**Lengsin is preferentially expressed in lung cancer cell lines and human primary lung cancer tissues.** Novel TAAs are essential for the establishment of cancer vaccine therapies. For the identification of novel TAAs, we initially screened the gene chip microarray expression profile database of more than 700 malignant tissues including breast, colon, pancreas, renal cell, lung and gastric carcinomas. We chose 30 cancer overexpressed genes as TAA candidates (data not shown). Then, the mRNA expression profiles of the TAA candidates were confirmed by RT-PCR, and one of the lung cancer-associated antigens proved to be the lens-specific GSI superfamily member, Lengsin. For precise analysis of Lengsin mRNA expression in various types of cancer cells RT-PCR analysis was performed with Lengsin primer pair I. As shown in Fig. 1(a), Lengsin was expressed in only three of the six lung cancer cell lines, but not in the two melanoma, four colorectal carcinoma, two breast carcinoma, four pancreas carcinoma and one hepatocellular carcinoma cell lines. To test the expression of Lengsin in the four major histological types of lung cancer, 12 lung cancer cell lines were examined by RT-PCR (Fig. 1b). Lengsin was expressed in one of the two squamous cell carcinoma lines (Sq-19), three of the five adenocarcinoma lines (LNY1, A549, 1-87), one large cell carcinoma line (86-2) and two of the four small cell carcinoma lines (Lu65, LK79). Then, we analyzed Lengsin expression in primary lung cancer tissue specimens. As shown in Fig. 1(c), we could detect Lengsin mRNA in primary lung cancerous tissues in 7 of the 7 (100%) cases, but not in normal counterpart tissues. The expression profile of Lengsin mRNA was also assessed in normal adult and fetal tissue panels including heart, brain, placenta, lung, liver, kidney, skeletal muscle, pancreas, spleen, thymus, prostate, testis, ovary, small intestine, large intestine and PBMCs (Fig. 1d). Lengsin mRNA could not be detected in mature adult tissues and fetal tissues with the exception of adult liver and placenta, although at very low levels. Thus, these data indicated that Lengsin mRNA was overexpressed specifically in primary lung cancer tissues as well as lung cancer cell lines with considerable frequency independent of the histological type, but not in major normal tissues.

**Novel Lengsin splicing variant 4 is the dominant form in lung cancer cell lines.** For precise analysis of the structure of Lengsin mRNA, we performed further RT-PCR analysis with an additional Lengsin primer pair located in the upstream of primer pair I (primer pair II, white arrow in Fig. 2a). As described above, we could detect a single band with primer pair I, whereas we detected two bands with primer pair II in lung cancer cell lines



doi: 10.1111/j.1349-7006.2009.01187.x

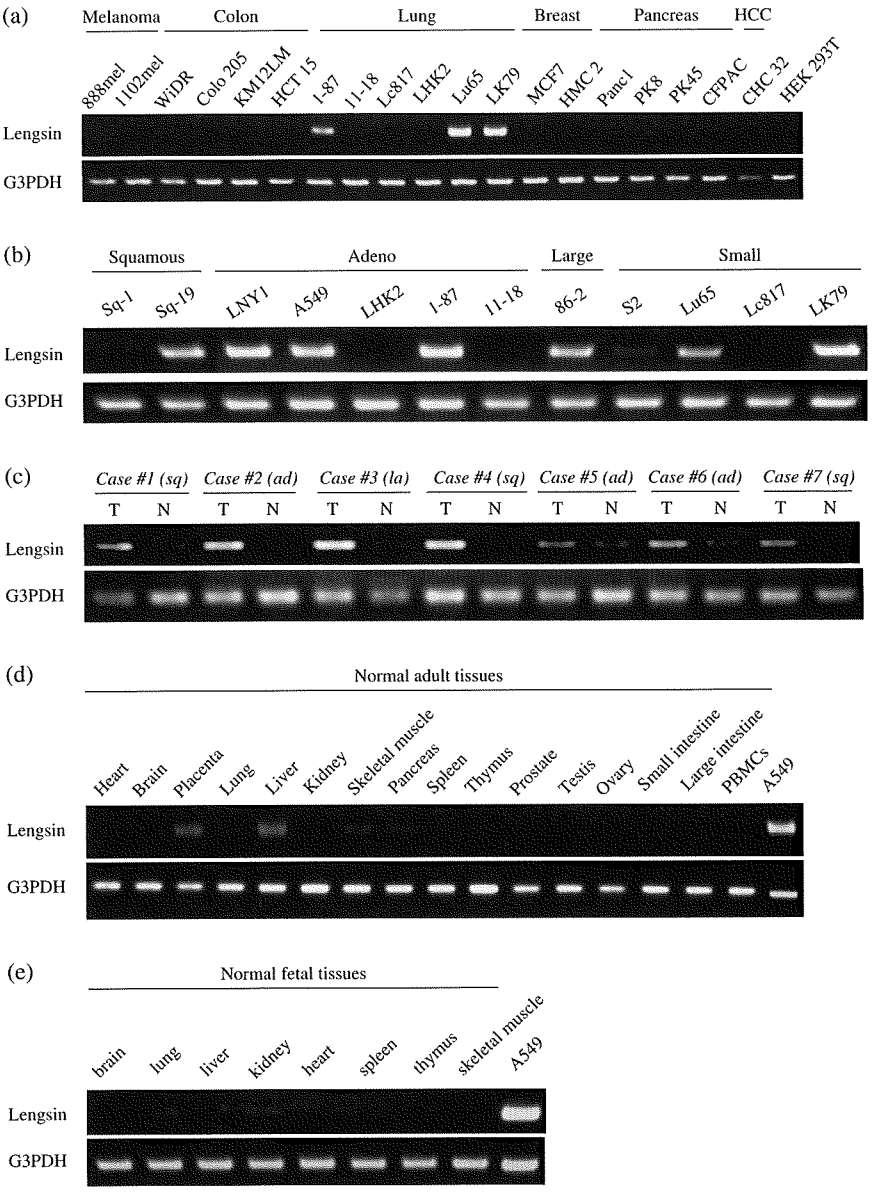


**Fig. 1.** Expression profiles of Lengsin as assessed by RT-PCR with Lengsin primer pair I in various cancer cell lines, lung cancer cell lines, human primary lung cancer tissues, normal adult tissues and fetal tissues. (a) Expression of Lengsin in various cancer cell lines. Cells include two melanoma cell lines (888mel, 1102mel), four colon cancer cell lines (WiDR, Colo205, KM12LM, HCT15), six lung cancer cell lines (1-87, 11-18, Lc817, LHK2, Lu65, LK79), two breast cancer cell lines (MCF7, HMC2), four pancreas cancer cell lines (Panc1, PK8, PK45, CFPAC), one hepatocellular carcinoma line (CHC32), and HEK293T. The expression of glyceraldehyde-3-phosphate dehydrogenase (G3PDH) was analyzed as an internal control. Melanoma, melanoma lines; Colon, colon cancer cell lines; Lung, lung cancer cell lines; Breast, breast cancer cell lines; Pancreas, pancreas cancer cell lines; HCC, hepatocellular carcinoma line. (b) Expression of Lengsin in lung cancer cell lines. Cells include two squamous cell carcinoma lines (Sq-1, Sq-19), five adenocarcinoma lines (LNY1, A549, LHK2, 1-87, 11-18), one large cell carcinoma line (86-2), and four small cell carcinoma lines (S2, Lu65, Lc817, LK79). Squamous, squamous cell carcinoma lines; Adeno, adenocarcinoma lines; Large, large cell carcinoma lines; Small, small cell carcinoma lines. (c) Expression of Lengsin in primary lung cancer (T) and non-cancerous tissues (N) including three squamous cell carcinomas (cases #1, #4, #7), three adenocarcinomas (cases #2, #5, and #6), and one large cell carcinoma (case #3). sq, squamous cell carcinoma; ad, adenocarcinoma; la, large cell carcinoma. (d) Expression of Lengsin in normal adult tissues and (e) fetal tissues, including heart, brain, placenta, lung, liver, skeletal muscle, kidney, pancreas, spleen, thymus, prostate, testis, ovary, small intestine, large intestine, and PBMCs. Lung adenocarcinoma line A549 was used as a positive control for Lengsin.

as shown in Fig. 2(c,d). With primer pair II, the estimated size of wild type Lengsin mRNA should be 395 bp, but the major band was located around 600 bp (Fig. 2d), suggesting the existence of a splicing variant. Therefore, we performed DNA direct sequencing of these two bands and found that the upper band corresponded to a novel spliced form, which we named splicing variant 4 (Lengsin_vt4), containing an additional exon 3 compared with the wild type (Fig. 2b). The lower weak band proved to be the wild-type form of Lengsin mRNA (Fig. 2b,d). Thus, these data indicated that a novel spliced form, Lengsin_vt4 was the major transcript in lung cancer cell lines.

**Detection of Lengsin protein in human lens and lung cancers by Western blot analysis and immunohistochemical staining.** To assess the Lengsin expression in lung cancer cells and tissues at the protein level, we generated novel anti-Lengsin mAb #517 suitable for Western blot analysis and immunohistochemical staining. The Lengsin-specific reactivity of mAb #517 was confirmed by Western blot analysis. We could detect a specific band with both anti-Lengsin mAb #517 and an anti-FLAG mAb in the HEK293T cell line transfected with expression vectors of FLAG-epitope-tagged Lengsin_vt4 (Fig. 3a), suggesting mAb #517 recognized Lengsin_vt4 protein specifically. The epitope of mAb #517 was located within exon 1 or exon 2 with further Western blot analysis using several deletion mutants (data not shown). Furthermore, we could detect Lengsin protein in human lens with mAb #517, but not with an isotype control mAb by immunohistochemical staining (Fig. 3b). Strong staining was seen in layers of secondary lens fibers, but not in the central region containing primary lens fibers (the lens nucleus). These findings are compatible with previous data of mouse Lengsin expression profiles.[7] The endogenously expressed Lengsin protein was also analyzed with Western blot analysis (Fig. 3c). The double-FLAG-tagged Lengsin_vt4 transfected 293T cells showed a specific band with mAb #517 as a positive control. A549 and 1-87 lung adenocarcinoma cell lines and LK79 small cell carcinoma line also showed mAb #517 specific band. Since these bands are located slightly lower than double FLAG tagged Lengsin_vt4 band, this difference might depend on the difference of double-FLAG-tag, which represents around 3 kDa. This protein expression profile was consistent with the mRNA expression. In addition, we performed immunohistochemical staining to assess the Lengsin protein expression *in vivo*. Thirty-four

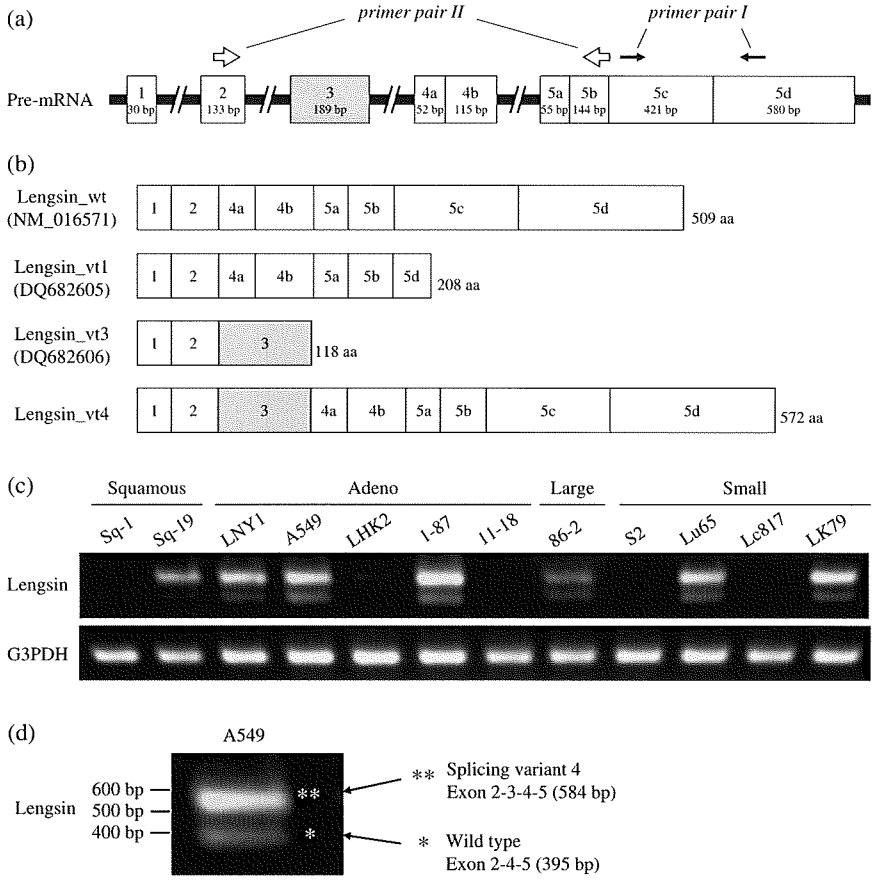


**Fig. 2.** Splicing variant 4 is more highly expressed than the wild type in lung cancer cell lines. (a) Diagram of premRNA showing five exons of Lengsin. Black arrow indicates PCR primer pair I and white arrow indicates PCR primer pair II. (b) Diagram of the derived protein of each splicing variant. Brackets indicate GenBank accession number. wt, wild type; vt1, splicing variant 1; vt3, splicing variant 3; vt4, splicing variant 4; aa, amino acid. (c) Expression profiles of Lengsin as assessed by RT-PCR with primer pair II in lung cancer cell lines. Squamous, squamous cell carcinoma lines; Adeno, adenocarcinoma lines; Large, large cell carcinoma lines; Small, small cell carcinoma lines. G3PDH was used as an internal control. (d) Results for two PCR products with primer pair II in A549.

surgically resected lung adenocarcinoma, 21 squamous cell carcinoma, two large cell carcinoma and four small cell carcinoma tissues were evaluated the expression of Lengsin proteins with mAb #517. Seventeen of 34 adenocarcinoma, 11 of 21 squamous cell carcinoma, two of two large cell carcinoma and two of four small cell carcinoma tissues showed positive staining (Table 1). In positive cases, Lengsin proteins could be detected in the cytoplasm of the cancer cells, but not in adjacent normal cells (Fig. 3d). To examine the expression of Lengsin protein in major normal tissues, we performed immunohistochemical staining with mAb #517. Lengsin protein was undetectable in liver and placenta, which expressed Lengsin mRNA at very low levels (Fig. 3e), or other organs including the heart, brain, lung, kidney, pancreas and large intestine (data not shown). These data suggest that Lengsin protein was preferentially expressed in lung carcinoma cells and secondary lens fibers, but not in major normal tissues including liver and placenta.

**Effect of Lengsin siRNA on cell viability in lung cancer cells.** To assess the functions of Lengsin protein in lung cancer cells, we investigated the effects of Lengsin siRNA on the survival of 1-87 cells, which expressed Lengsin, by WST-1 assay and flow cytometric analysis. Introducing Lengsin-specific siRNA significantly reduced expression of Lengsin mRNA compared with control siRNA (Fig. 4a). WST-1 assay revealed that treatment with Lengsin siRNA significantly decreased the cell viability compared with control siRNA (Fig. 4b,c). In addition, we measured the percentage of sub-G1 cells, which represents the percentage of apoptotic cells, by flow cytometric analysis using PI staining of DNA. The percentage of apoptotic cells was found to be increased in Lengsin siRNA-treated cells (Fig. 4d). These data indicate that Lengsin might be essential for cell viability in Lengsin-positive lung cancer cells.

**Table 1. Clinical characteristics of patients with lung cancer and detection of Lengsin protein by immunohistochemical staining**

| Histology | Positive/total | | | |
|---|---|---|---|---|
| | Adeno | Squamous | Large | Small |
| Patients | 17/34 (50%) | 11/21 (52%) | 2/2 (100%) | 2/4 (50%) |
| Age (years) | | | | |
| < 65 | 8/16 | 2/6 | 1/1 | 2/3 |
| > 65 | 9/18 | 9/15 | 1/1 | 0/1 |
| Sex | | | | |
| Male | 7/14 | 10/20 | 2/2 | 0/2 |
| Female | 10/20 | 1/1 | ND | 2/2 |
| UICC Stage | | | | |
| Stage I | 10/27 | 4/11 | 1/1 | 1/2 |
| Stage II | 1/1 | 3/3 | ND | ND |
| Stage III | 6/6 | 4/7 | 1/1 | 1/1 |
| Stage IV | ND | ND | ND | 0/1 |

Adeno, adenocarcinoma; Squamous, squamous cell carcinoma; Large, large cell carcinoma; Small, small cell carcinoma; ND, not determined.

**Detection of anti-Lengsin autoantibodies by ELISA.** Since Lengsin protein is expressed only in cancerous tissue and the normal lens, which is an immunologically privileged site, we hypothesized that Lengsin might be one of the immunogenics for immune systems. Thus, to assess the immune response against Lengsin *in vivo* we investigated anti-Lengsin autoantibodies in sera from 23 lung cancer patients and 19 healthy donors by ELISA using recombinant Lengsin protein. The cutoff value was settled as the


doi: 10.1111/j.1349-7006.2009.01187.x

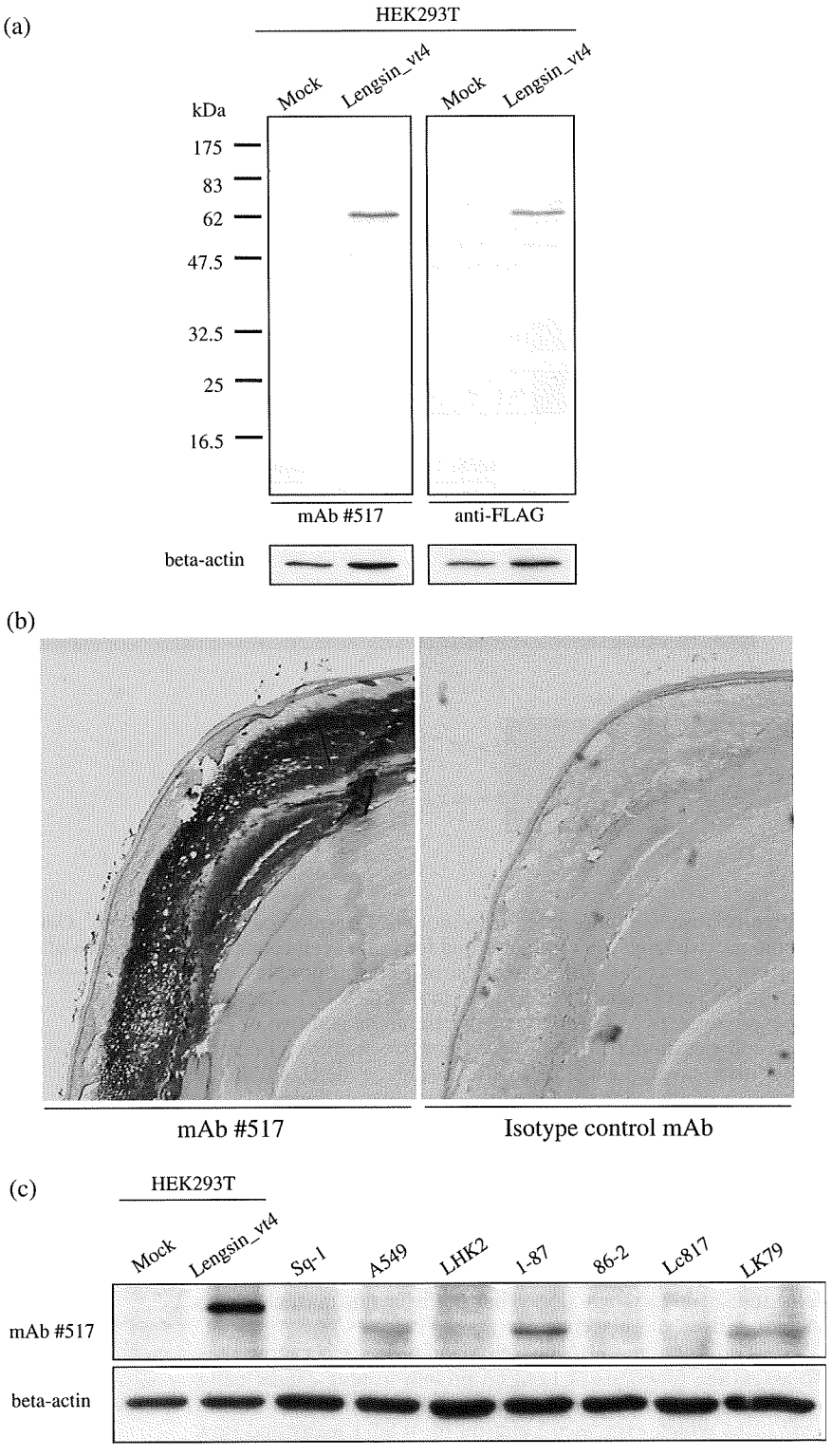


**Fig. 3.** Detection of Lengsin protein as assessed by Western blot analysis and immunohistochemical staining with anti-Lengsin mAb #517. (a) Specific detection of Lengsin protein in HEK293T cells transfected with expression vectors of FLAG-epitope-tagged Lengsin_vt4 as assessed by Western blot analysis with mAb #517 and an anti-FLAG mAb. Beta-actin was used as a protein loading control. (b) Detection of Lengsin in human lens by immunohistochemical staining with mAb #517. Magnification 40×. (c) Expression of Lengsin in lung cancer cell lines as assessed by Western blot analysis. HEK293T cells transfected with Lengsin_vt4 or mock-transfected were used as a control sample. (d) Representative immunohistochemical staining with mAb #517 in primary lung adenocarcinoma, squamous cell carcinoma, large cell carcinoma and small cell carcinoma tissues. Magnification 200×. (e) Representative immunohistochemical staining with mAb #517 in normal liver and placenta. Magnification 200×.

mean plus two SD of healthy donor samples. The clinical characteristics and results of 23 lung cancer patients are summarized in Table 2. There is no significant difference of anti-Lengsin antibodies between healthy donors and lung cancer patients; sera from 6 of the 23 lung cancer patients (26.1%) were positive. These data indicated that the anti-Lengsin immune response was elicited with Lengsin protein ectopically expressed in lung cancer cells. Moreover, all six anti-Lengsin autoantibody-positive patients had no oculopathy including any disease of the lens, indicating that anti-Lengsin antibodies might not be relevant to a lens-related pathologic state. Anti-Lengsin autoantibodies in serum might have no adverse effect on the ocular compartment, which is presumed to be an immune-privileged site. Taken together, these results strongly suggest that ectopically expressed Lengsin could cause immunological reactions for lung cancer cells, but not for the lens; hence, Lengsin might be a novel target molecule for cancer immunotherapy as well as for a diagnostic marker.

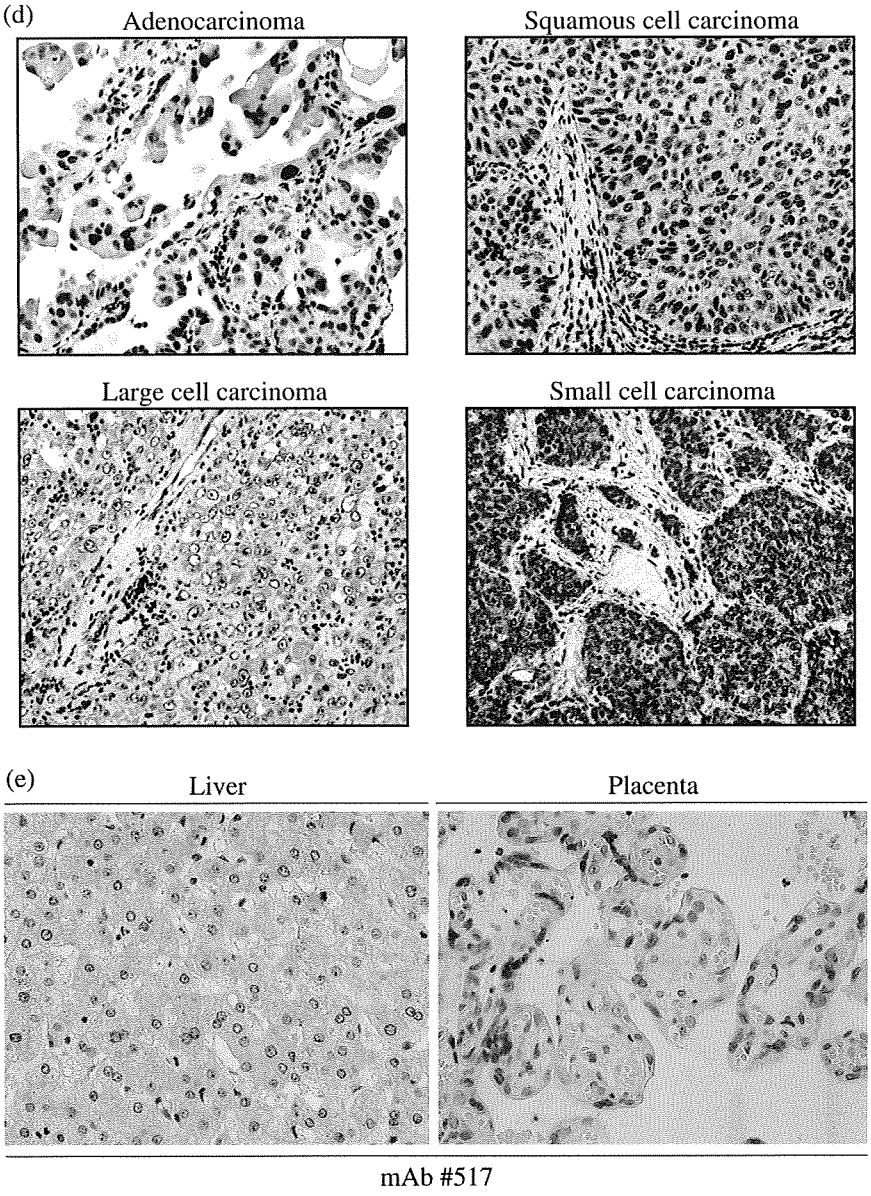


**Fig. 3.** *Continued.*

## Discussion

Wistow *et al.* reported that Lengsin was an abundant transcript in the human lens, and had a sequence similar to glutamine synthetase.[13] However, Lengsin did not catalyze glutamine synthesis, yet cross-reacted with antiglutamine synthetase antibodies assembled into the same dodecameric structure as prokaryotic class I glutamine synthetase.[5,6]

Lengsin is a highly specific protein for the lens.[5–7] Lengsin and lens intermediate filament proteins colocalize at the plasma membrane in maturing lens fiber cells and expression of Lengsin correlates with the reorganization of the lens fiber cell cytoskeleton. Thus, it may act as a component of the cytoskeleton in the lens.[7] In addition, Lengsin was expressed at high levels in the transparent but not the cataractous human lens, indicating that it may be related to the maintenance of lens transparency. Moreover, Lengsin relieves cellular toxicity caused by amyloid-beta expression, and thus, may have a chaperone-like role.[5]

In this study, we reported for the first time that Lengsin, a novel lung cancer antigen, was overexpressed ectopically in the four major histological types of lung cancer. Furthermore, we could immunohistochemically detect Lengsin protein strongly in the human lens with anti-Lengsin mAb #517 generated in our study. Lengsin protein was detected in 50–100% of primary lung carcinoma tissues with mAb #517, but was not detectable in any normal tissues except for lens. Thus, mAb #517 might be a fine marker to diagnose lung carcinoma and define the indication for molecular targeting therapy using Lengsin.

Two splicing variants of Lengsin, variants 1 and 3, were already reported to be expressed in the human lens.[5] Analysis of the gene structure of Lengsin in lung cancer cells revealed that a new splicing variant of human Lengsin mRNA, which was termed splicing variant 4 (Lengsin_vt4), was the major transcript in lung cancer cells. Lengsin_vt4 retains exon 3 that codes 63 amino acids between exon 2 and exon 4 without the frame shift, but the wild type of human Lengsin does not contain exon 3. Lengsin protein retains exon 3 in mammals other than primates.[6] Exon 3 might be evolutionarily eliminated in the human lens; however, our data indicated that Lengsin_vt4 retaining exon 3 was expressed dominantly in human lung cancer cells.

In addition, knockdown of Lengsin expression caused a decrease of cell viability in 1-87 cells, which expressed Lengsin.



doi: 10.1111/j.1349-7006.2009.01187.x

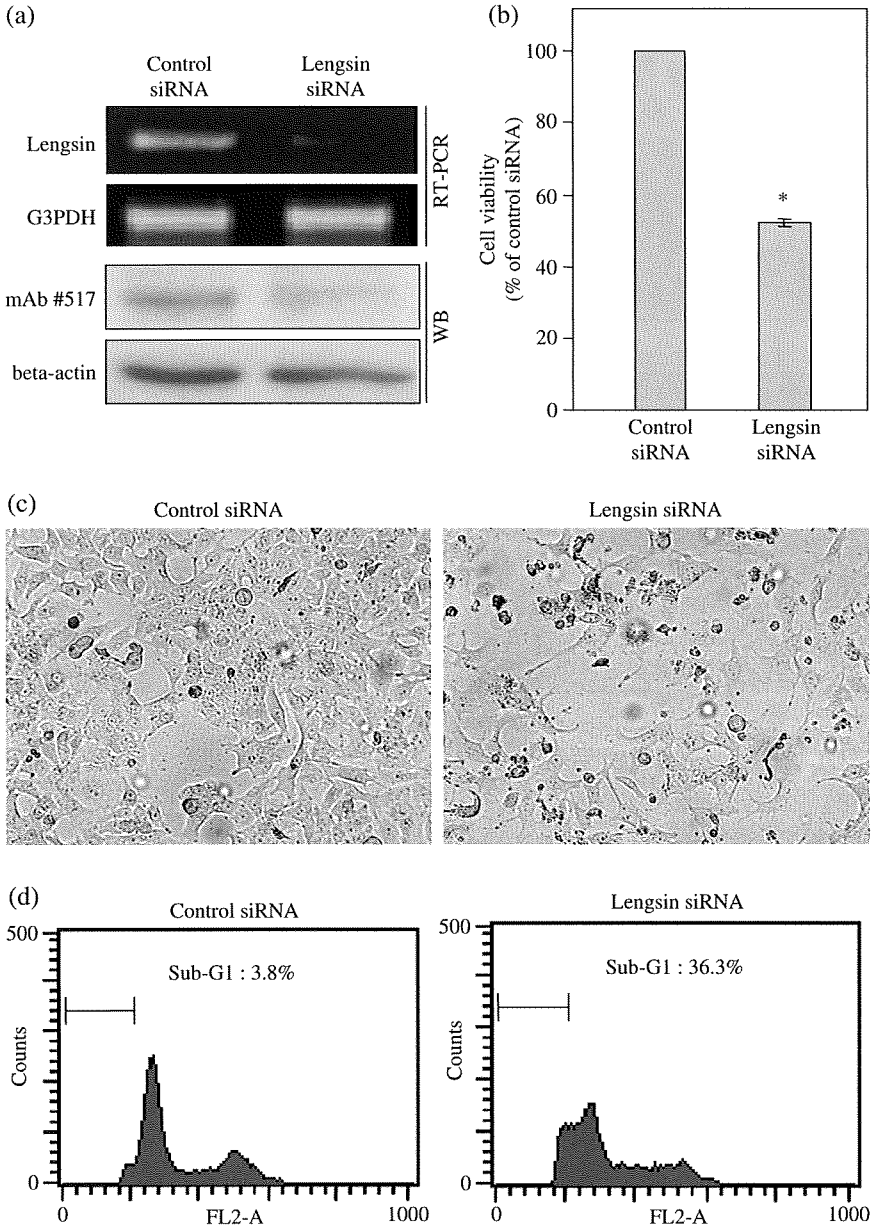


**Fig. 4.** Effect of Lengsin on cell viability in lung cancer cell line 1-87. (a) Gene silencing was performed using Lengsin siRNA. RT-PCR analysis was done using Lengsin primer pair I. G3PDH was used as an internal control. (b) WST-1 assay shows a decrease in the numbers of viable cells after knockdown of Lengsin expression in 1-87 cells. Statistical analysis was done using a Student's *t*-test. *, $P < 0.01$ compared with the control siRNA. The assay was performed in triplicate; bars, SD. (c) 1-87 cells transfected with control siRNA (right panel) and Lengsin siRNA (left panel). Magnification, ×200. (d) Percentage of cells in the sub-G1 phase indicated by bars was determined by flow cytometry using propidium iodide staining of DNA.

Although the mechanism remains unclear, Lengsin might play an essential role for cell viability in Lengsin-expressing cancer cells.

It remains to be explained why a lens-specific protein is expressed in lung cancers. The eye, including the retina and lens, is considered an immune-privileged site and is protected from immune responses by a variety of mechanisms including the blood–organ barrier, lack of lymphatic drainage, low expression of MHC molecules, local production of immunosuppressive cytokines such as TGF-beta and constitutive expression of Fas ligand.[14,15] However, recoverin, a calcium-binding protein localized specifically in the retina, is expressed in various cancers,[16,17] and it is reported that antirecoverin autoantibodies may cause retina cells to degenerate and cause cancer-associated retinopathy.[18,19] This suggests the retina is an incompletely immune-privileged organ. Immunization of recoverin-positive cancer-bearing mice with recoverin-derived antigenic peptide caused both an antitumor effect and dysfunction of the retina.[20] On the other hand, no lens-related disease caused by an autoimmune response against any cancer antigen has been reported to date. Our data also showed that antilengsin antibody positive lung cancer patients had no lens troubles, suggesting that the lens is completely immune-privileged, which is different from the retina. As Lengsin localizes to the cytosol, anti-Lengsin antibodies might not have biological significance; however, Lengsin protein derived from necrotic or apoptotic cancer cells can make immune complexes with anti-Lengsin antibody, which can potentially cause serial immunological responses including CTL activity and subsequent injury of the lens. However, our data suggest that the anti-Lengsin immunological response is not harmful for the lens, and support the feasibility of lung cancer immunotherapy targeting the Lengsin molecule.

The testis is also an immune-privileged site.[21] It is well known that cancer–testis (CT) antigens, including the MAGE gene family and NY-ESO-1, are expressed exclusively in cancers and normal testis tissue. Hence, it is difficult to induce immune tolerance toward CT antigens.[22] Therefore, CT antigens are highly immunogenic and are promising targets for cancer immunotherapy.[23–25]

| Patient No. | Sex | Age | Histology | UICC Stage | Anti-Lengsin autoantibodies† | Lengsin‡ |
|---|---|---|---|---|---|---|
| 1 | Male | 61 | Ad | IIIB | + | + |
| 2 | Male | 79 | Ad | IA | + | + |
| 3 | Female | 79 | Ad | IV | + | ND |
| 4 | Male | 76 | Sq | IB | + | + |
| 5 | Female | 65 | Ad | IA | + | + |
| 6 | Male | 60 | Sq | IIIA | + | + |
| 7 | Male | 67 | Ad | IV | – | ND |
| 8 | Male | 59 | Sq | IA | – | – |
| 9 | Male | 65 | Ad | IA | – | + |
| 10 | Female | 62 | Ad | IIIB | – | ND |
| 11 | Male | 63 | Ad | IV | – | ND |
| 12 | Male | 87 | Ad | IV | – | ND |
| 13 | Male | 70 | Ad | IA | – | + |
| 14 | Female | 64 | Sm | IB | – | + |
| 15 | Male | 65 | Sq | IIIB | – | ND |
| 16 | Male | 69 | Sq | IA | – | + |
| 17 | Male | 66 | Ad | IIIB | – | + |
| 18 | Male | 62 | Sm | IA | – | – |
| 19 | Male | 73 | Sq | IIA | – | – |
| 20 | Male | 74 | Ad | IA | – | + |
| 21 | Male | 56 | Ad | IA | – | – |
| 22 | Male | 73 | Sm | IV | – | – |
| 23 | Female | 56 | Ad | IA | – | – |

**Table 2. Clinical characteristics of serum donors with lung cancers and detection of anti-Lengsin autoantibodies by ELISA**

Ad, adenocarcinoma; ELISA, enzyme-linked immunosorbent assay; Sq, squamous cell carcinoma; Sm, small cell carcinoma; ND, not determined.
†The cutoff value is the mean plus two SD for healthy donor samples. Antibody levels for upper or lower cutoff values are evaluated as either positive (+) or negative (–), respectively.
‡Positive (+) or negative (–) indicate that expression of Lengsin protein in lung cancer tissues assessed by immunohistochemical staining is either detected or not detected, respectively.

Lengsin is expressed exclusively in lung cancers and the immune-privileged normal lens; thus, we consider Lengsin to be not only a risk-free but also a highly immunogenic target for immunotherapy. We are now investigating and identifying Lengsin epitopes recognized by cytotoxic T lymphocytes. Some cancer–testis antigens have been isolated by analyzing a testis cDNA expression library with cancer patients' sera.[26–28] Possible new cancer antigens like Lengsin, which is exclusively expressed in the lens and cancer, may be found by studying a lens cDNA library. Lengsin is obviously the first such reported cancer antigen, a 'cancer–lens antigen', which might play a role in molecular targeting therapy, including antigen-specific immunotherapy like cancer–testis antigens.

In summary, we identified that lens-specific antigen Lengsin is expressed ectopically in lung cancer cells. The predominant transcript form was a novel splicing variant, termed Lengsin_vt4. Lengsin plays an essential role in lung cancer cell survival. Anti-Lengsin humoral immune reactions could be detected in lung cancer patients' serum, but not in healthy donors'. These data suggest that Lengsin_vt4 might be a novel biomarker of lung cancers, and also a molecular target including immunotherapy.

## Acknowledgments

Thanks to Drs K Imai, K Itoh, BJ van den Eynde, PG Coulie and K Kuzushima for kindly providing cell lines and S Ottonello for kindly providing the plasmid of Lengsin. This study was supported by a Grant-in-Aid for Scientific Research from the Ministry of Education, Culture, Sports, Science and Technology in Japan.

## Disclosure statement

There is no financial interest with regard to the submitted manuscript that might be construed as a conflict of interest.

## Abbreviations

| | |
|---|---|
| mAb | monoclonal antibody |
| PBMCs | peripheral blood mononuclear cells |
| RT-PCR | reverse transcription-PCR |
| TAA | tumor-associated antigen |
| UICC | International Union Against Cancer |

## References

1 American Cancer Society. *Cancer Facts and Figures*. Atlanta, GA: American Cancer Society, 2007.
2 Brunsvig PF, Aamdal S, Gjertsen MK *et al*. Telomerase peptide vaccination: a phase I/II study in patients with non-small cell lung cancer. *Cancer Immunol Immunother* 2006; **55**: 1553–64.
3 Oka Y, Tsuboi A, Taguchi T *et al*. Induction of WT1 (Wilms' tumor gene) – specific cytotoxic T lymphocytes by WT1 peptide vaccine and the resultant cancer regression. *Proc Natl Acad Sci USA* 2004; **101**: 13 885–90.
4 Golub TR, Slonim DK, Tamayo P *et al*. Molecular classification of cancer: class discovery and class prediction by gene expression monitoring. *Science* 1999; **286**: 531–7.
5 Grassi F, Moretto N, Rivetti C *et al*. Structural and functional properties of lengsin, a pseudo-glutamine synthetase in the transparent human lens. *Biochem Biophys Res Commun* 2006; **350**: 424–9.
6 Wyatt K, White HE, Wang L *et al*. Lengsin is a survivor of an ancient family of class I glutamine synthetases re-engineered by evolution for a role in the vertebrate lens. *Structure* 2006; **14**: 1823–34.
7 Wyatt K, Gao C, Tsai JY *et al*. A role for lengsin, a recruited enzyme, in terminal differentiation in the vertebrate lens. *J Biol Chem* 2008; **283**: 6607–15.
8 Mountain CF. Revisions in the international system for staging lung cancer. *Chest* 1997; **111**: 1710–7.



doi: 10.1111/j.1349-7006.2009.01187.x